Quaternary Science Reviews 122 (2015) 233–249

Contents lists available at ScienceDirect

Quaternary Science Reviews

journal homepage: www.elsevier.com/locate/quascirev

# Radiocarbon chronology of the last glacial maximum and its termination in northwestern Patagonia

Patricio I. Moreno [a, *], George H. Denton [b], Hugo Moreno [c], Thomas V. Lowell [d], Aaron E. Putnam [b, e], Michael R. Kaplan [e]

[a] Department of Ecological Sciences, Millennium Institute of Ecology and Biodiversity, Center for Climate Research and Resilience, and Millennium Nucleus Paleoclimate of the Southern Hemisphere, Universidad de Chile, Santiago, Chile
[b] School of Earth and Climate Sciences and Climate Change Institute, University of Maine, Orono, ME 04469, USA
[c] Observatorio Volcanológico de los Andes del Sur, Servicio Nacional de Geología y Minería, Temuco, Chile
[d] Department of Geology, University of Cincinnati, Cincinnati, 500 Geology/Physics Building, Cincinnati, OH 45221, USA
[e] Lamont-Doherty Earth Observatory of Columbia University, Palisades, NY, USA

ARTICLE INFO

*Article history:*
Received 16 March 2015
Received in revised form
27 May 2015
Accepted 28 May 2015
Available online 16 June 2015

*Keywords:*
*Nothofagus* rise
North Patagonian rainforests
Llanquihue moraines
Licán ignimbrite
Northwestern Patagonia
Southern mid-latitudes
Last glacial maximum
Last glacial termination
Heinrich Stadial 1

ABSTRACT

We examine the timing and magnitude of the last glacial maximum (LGM) and the last glacial termination (LGT) in northwestern Patagonia, situated in the middle latitudes of South America. Our data indicate that the main phase of the LGT began with abrupt warm pulses at 17,800 and 17,100 cal yrs BP, accompanied by rapid establishment of evergreen temperate rainforests and extensive deglaciation of the Andes within 1000 years. This response shows that South American middle-latitude temperatures had approached average interglacial values by 16,800 cal yrs BP. The temperature rise in northwestern Patagonia coincides with the beginning of major warming and glacier recession in the Southern Alps of New Zealand at southern mid-latitudes on the opposite side of the Pacific Ocean. From this correspondence, the warming that began at 17,800 cal yrs BP appears to have been widespread in middle latitudes of the Southern Hemisphere, accounting for at least 75% of the total temperature recovery from the LGM to the Holocene. Moreover, this warming pulse is coeval with the first half of the Heinrich Stadial 1 (HS1) in the North Atlantic region. HS1 featured a decline of North Atlantic meridional overturning circulation, a southward shift of the westerly wind belt in both hemispheres and of the Intertropical Convergence Zone, as well as a weakening of the Asian monsoon. Along with the initiating trigger, identifying the mechanisms whereby these opposing climate signals in the two polar hemispheres interacted —whether through an oceanic or an atmospheric bipolar seesaw, or both— lies at the heart of understanding the LGT.



## 1. Introduction

Terminations of ~100,000-year glacial cycles represent the largest natural climate changes of late-Quaternary time. Terminations set the overall timing of these cycles by disrupting the evolution of the global climate system toward extreme glacial conditions. They feature melting of huge continental ice sheets situated in the Northern Hemisphere, together with reorganization of the global ocean-atmosphere system from a glacial to an interglacial mode. Deciphering the mechanisms responsible for terminations is thus prerequisite for understanding the causes of ~100,000-year glacial cycles. Discussion of this topic has centered largely on the phasing relationships of climate events revealed in polar ice cores, which show interhemispheric asynchrony in the millennial bandwidth (Members, 2015). The extent to which these ice-core records are representative of climate change in extra-polar areas is insufficiently understood. To address this problem, we present radiocarbon-dated terrestrial stratigraphic records from northwestern Patagonia and compare them with the glacier and vegetation record in the Southern Alps of New Zealand, both situated in southern middle latitudes. Precisely dated stratigraphic records from the southern middle latitudes afford a test of the hemispheric-scale significance of the climate signature of Antarctic

* Corresponding author.
*E-mail addresses:* pimoreno@uchile.cl (P.I. Moreno), gdenton@maine.edu (G.H. Denton), hmoreno@sernageomin.cl (H. Moreno), thomas.lowell@uc.edu (T.V. Lowell), mkaplan@ldeo.columbia.edu (M.R. Kaplan).

http://dx.doi.org/10.1016/j.quascirev.2015.05.027
0277-3791/

ice cores, and may clarify the relative roles of changes in deep-water circulation and/or shifts in major wind belts for the initiation and propagation of abrupt climate changes at global scales, including those associated with the last glacial termination (LGT).

Our radiocarbon-dated palynologic and glacial geologic records come from the lowlands of northwestern Patagonia in the Chilean Lake District, Isla Grande de Chiloé and on the adjacent Chiloé Continental sector (Fig. 1). Our collation of new and published AMS (Accelerator Mass Spectrometry) $^{14}$C-dated terrestrial records allows us to define the timing and sequence of events during the last glacial maximum (LGM) and the LGT in the middle latitudes alongside the southeastern Pacific Ocean. Our aim is to examine the intra- and inter-hemispheric phasing of paleoclimate signals during the LGT. For that purpose we developed a master pollen stratigraphy that combines the palynology and associated radiocarbon dates from sites with high-resolution records, together with radiocarbon-dated volcanic and glacial deposits and geomorphic features that are key to deciphering the timing and extent of Andean ice lobes during the LGM and the LGT. Our radiocarbon chronology relies on terrestrial samples, which directly monitor the radiocarbon content of the atmosphere, thus circumventing the uncertainties of changing marine reservoir corrections.

## 2. Setting

Northwestern Patagonia (40°–44°S) features the Chilean Lake District and the Chilotan archipelago, most noteworthy Isla Grande de Chiloé (Fig. 1). It is bounded by the Andes Cordillera in the Chiloé Continental sector in the east and by the Coastal Range in the west that runs along a north-to-south axis adjacent to the southeastern sector of the Pacific Ocean. The overall cordillera attains its highest altitudes between 15° and 35°S, with maximum elevations declining steadily toward the south (~2500 m.a.s.l. at 35°S, ~1800 m.a.s.l. at 40°S, and ~1400 m.a.s.l. at 45°S). Abundant precipitation delivered by westerly winds coupled with adiabatic cooling allows the occurrence of more than 35 isolated glaciers on the highest peaks between 35° and 45°30′S (Lliboutry, 1998), most of them volcanoes. Cirque glaciers become increasingly common poleward of 41°S, followed south of 45°30′S by numerous mountain glaciers, outlet glaciers, and ice fields, including the Northern and Southern Patagonian Ice Fields. The calculated equilibrium line altitude declines poleward from elevations of ~3300 m.a.s.l. at 35°S, to ~2300 m.a.s.l. at 40°S, to a minimum of ~600 m.a.s.l. at 52°S (Condom et al., 2007).

Northwestern Patagonia is under the influence of explosive eruptions from several volcanoes in the Southern Andean Volcanic Zone. This volcanism results from the subduction of the Nazca Plate beneath the westward moving South American Plate (Stern, 2004), along a narrow volcanic arc that follows the Liquiñe-Ofqui fault system in Chile between 33° and 46°S. The Southern Andean Volcanic Zone includes at least 60 active or potentially active volcanoes in Chile and Argentina, as well as three caldera systems and numerous minor eruptive centers (Stern, 2004). Several active volcanoes have historic explosive records. The most relevant are Mocho-Choshuenco (39°55′39″S, 72°1′37″W), Lanín (39°37′58″S, 71°29′59″W), Grupo Antillanca (40°46′15″S, 72°9′12″W), Osorno (41°6′0″S, 72°29′35″W), the recently erupted Puyehue-Cordón Caulle (40°35′25″S, 72°7′2″W) and Volcán Chaitén (42°49′58″S, 72°38′45″W) on years 2011 and 2008 respectively, and the currently active Volcán Villarrica (39°25′0″S, 71°56′0″W) and V. Calbuco (41°19′34″S, 72°36′52″W).

Precipitation of westerly origin occurs throughout the year in northwestern Patagonia, with variations in frontal activity resulting from latitudinal shifts of storm tracks at seasonal and interannual scales (Garreaud et al., 2013). The seasonality of precipitation increases north of 41°S, along with a rise in continentality caused by the rain-shadow effect of the Coastal Range on the Longitudinal Valley, a broad north-south oriented tectonic depression situated between the Coastal Range and the Andes Cordillera. The zone of maximum precipitation (48°–50°S in central Patagonia) shifts north/south during the winter/summer months, respectively, along with latitudinal sea-surface temperature gradients and the interaction between the subtropical Pacific high-pressure cell and the polar low-pressure belt (Aceituno et al., 1993; Garreaud et al., 2013; Quintana and Aceituno, 2012).

The temperate high-rainfall regime in northwestern Patagonia fosters broadleaved temperate rainforests, which closely follow altitudinal and latitudinal climate gradients in temperature and precipitation from sea level up to the treeline (1000–1200 m.a.s.l.). The upper treeline represents a major discontinuity in the distribution of arboreal species in the cold, wet, and wind-swept environments of the high Andes of Patagonia. A study of the spatial and temporal variation in *Nothofagus pumilio* growth at treeline along its latitudinal range (35°40′S-55°S) in the Chilean Andes (Lara et al., 2005) showed that (i) temperature has a spatially larger control on tree growth than precipitation, and that (ii) this influence is particularly significant in the temperate Andes (>40°S). These results suggest that low temperatures are the main limiting factor for the occurrence of woodlands and forests at high elevations in the Andes, considering that precipitation increases with elevation at any given latitude (Lara et al., 2005).

The temperate rainforests in northwestern Patagonia are dominated or co-dominated by species of the genus *Nothofagus*, the Southern Beech. These rainforests occur from sea level onto the humid slopes of the western flanks of the Andes and Coastal Range (Fig. 1) (Villagrán, 1985, 1988a, b). Between 40° and 43°S, three main forest communities have been distinguished on the basis of their floristic composition: Valdivian, North Patagonian, and Subantarctic. The evergreen Valdivian rainforest, the most biodiverse and heterogeneous in terms of canopy structure, occupies low-elevation sectors in relatively warm areas with strong precipitation seasonality and inter-annual variability in the northern part of this region. Important pollen indicators characterize the modern pollen rain of this forest community, among them are the trees *Eucryphia cordifolia* and *Caldcluvia paniculata*, accompanied by numerous other trees, shrubs, epiphytes, and vines. North Patagonian evergreen rainforests supersede or intermingle with Valdivian communities under colder/wetter conditions, either upslope in the mountain ranges in northwestern Patagonia or in areas south of 41°S. The Valdivian and North Patagonian communities share many species, the latter having lower biodiversity and a simpler canopy structure, together with the presence and occasional dominance of cold-resistant conifers (*Podocarpus nubigena*, *Saxegothaea conspicua*, *Fitzroya cupressoides*, and *Pilgerodendron uviferum*) at higher elevations (550–850 m.a.s.l.) and in Isla Grande de Chiloé. Deciduous Subantarctic forests dominate sub-alpine environments subject to seasonal snow cover under cold, wet, and windy conditions. The broad latitudinal distribution of the Subantarctic forest community throughout western Patagonia reflects its ability to withstand extreme temperature conditions. These winter-deciduous forests establish a transition between the evergreen rainforests discussed above and the Patagonian Steppe east of the Andes, and the High Andean plant communities located above the treeline. The dominant species in Subantarctic forests is *N. pumilio*, which may form monospecific stands and present a species-poor understory. *N. pumilio* forests intermingle with *Nothofagus betuloides* in more humid sectors, establishing a mosaic with evergreen forests. In palynological terms, this plant community can be traced by assemblages having an arboreal component dominated almost exclusively by *Nothofagus* pollen, lacking epiphytes and vines, and

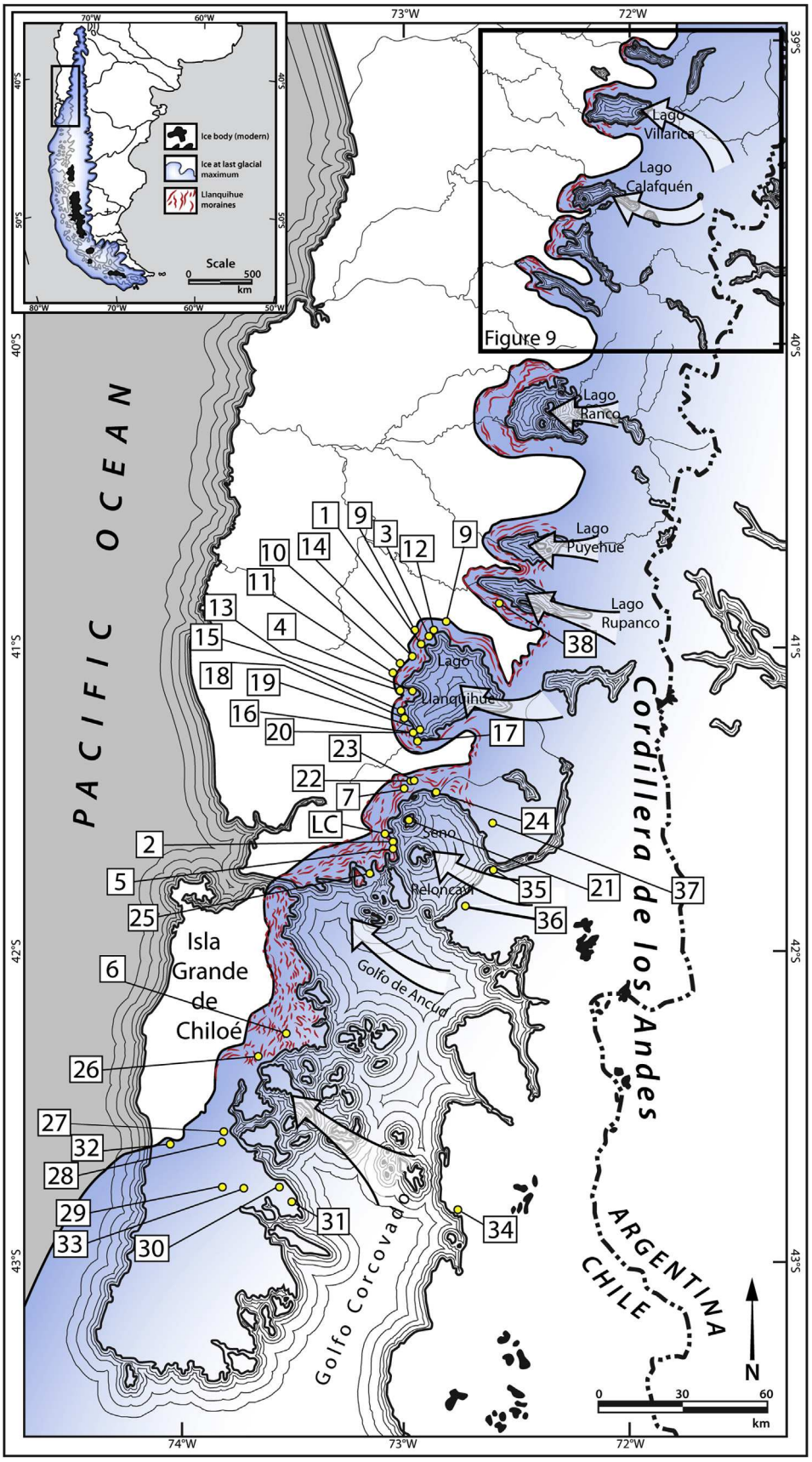


**Fig. 1.** Map of the study area showing the location of palynological (Canal de la Puntilla: 1, Huelmo: 2, Lago Condorito = LC, Lago Lepué: 23) and stratigraphic sites discussed in the text. Also shown are the mapped moraines west of the major lakes and gulfs, along with the reconstructed extent of Andean piedmont ice lobes during the last glacial maximum.

featuring understory herbs and shrubs (Apiaceae, *Valeriana*, *Perezia*, *Lycopodium magellanicum*, *Huperzia selago*, etc.). Evergreen subantarctic forests dominated by *N. betuloides* transition into Magellanic Moorland communities in the windswept, hyperhumid, low-permeability rocky substrates of the Chilean channels.

High Andean vegetation dominates the landscapes above the treeline, located between 1000 and 1200 m elevation in northwestern Patagonia, and constitutes a sparsely vegetated unit dominated by herbs (Poaceae [*Poa*, *Festuca*, *Deschampsia*], Asteraceae [*Nassauvia*, *Senecio*, *Perezia*], Apiaceae [*Bolax*, *Azorella*], Cyperaceae [*Carex*], *Gunnera*), and shrubs (Ericaceae [*Gaultheria*], *Empetrum*), along with isolated individuals of the species *Nothofagus antarctica*. Low temperatures, strong winds, and prolonged and abundant snow cover constitute limiting factors for the occurrence of woodlands and forests in this harsh environment.

The interaction of the physical and biological characteristics of northwestern Patagonia led to the repeated formation of a large Patagonian Ice Sheet during late-Quaternary ice ages, accompanied by geographic shifts of the land biota, including floristic and physiognomic changes in the regional plant communities. Several aspects make this region particularly suitable for deciphering the timing, rate, and magnitude of paleoclimate changes during the LGM and the LGT:

A. Numerous lakes and bogs located in topographic depressions and in meltwater channels are associated with moraine complexes deposited during Marine Isotope Stages (MIS) 2–4 (Denton et al., 1999b), thus allowing the development of stratigraphic records before, during, and since the LGM. Furthermore, glaciers advanced over vegetated landscapes, overriding organic-rich surfaces such as andesitic soils, lacustrine beds, peat, and forest beds, thus offering the opportunity to define the timing of glacial advances by radiocarbon dating (Denton et al., 1999b; Mercer, 1968, 1976; Porter, 1981). The abundance of organic-rich, high-sediment-accumulating lake basins dating to the last glaciation enables the development of the high-resolution paleoecological records necessary to infer past paleoclimate shifts, as well as treeline and snowline fluctuations.
B. Extensive areas in northwestern Patagonia remained ice-free during the last glaciation (Denton et al., 1999b; Laugenie, 1982; Mercer, 1968, 1976; Porter, 1981), allowing biota to occupy the northeastern portion of Isla Grande de Chiloé (Heusser, 1990; Villagrán, 1990, 2001) and the well-drained proglacial outwash substrates in the Longitudinal Valley of the Chilean Lake District (Heusser, 1974; Heusser et al., 1999, 1996a; Moreno, 1997) (Fig. 1) under cold, wet, and windy conditions. The fact that the glacial vegetation thrived near former glacier margins allowed a rapid spread of cold-resistant pioneer herbs, shrubs, and trees into the lowlands of the Chilean Lake District at the end of the LGM (Heusser et al., 1996a; Moreno, 1997). Hence, palynological records from this area can monitor the local response of the vegetation to the very early stages of the LGT, devoid of biases introduced by seaway barriers to dispersal, migrational lags, and soil development in recently deglaciated terrain, as well as by climate heterogeneities at regional to continental scales (Bennett et al., 2000; Moreno et al., 2001).
C. The relatively high species richness associated with the rainforest and high Andean communities in northwestern Patagonia, together with the segregation of these communities along the climate gradients discussed above, permits detection of major physiognomic shifts as well as subtle changes in the composition of the vegetation inferred from fossil pollen records (Moreno, 2004; Pesce and Moreno, 2014).
D. Large explosive volcanic events during and since the LGM resulted in the deposition of pyroclastic layers that mantle glacial and non-glacial landforms (Clavero and Moreno, 2004; Singer et al., 2008), which constitute the substrate for the development of organic deposits in former wetlands or soils. Radiocarbon dating of these volcanic deposits, some of which are areally extensive, enables the development of detailed chronologies to constrain the timing of glacial fluctuations and deglaciation.

## 3. Methods

Our radiocarbon-dated signature for the LGM and LGT in northwestern Patagonia is based on the timing of vegetation changes revealed by pollen sequences, and of glacier maxima during the LGM, followed by recession from LGM moraine belts. We discuss each of these in turn. The high-resolution palynology shown in this study comes from sediment cores collected from two mires located in the Chilean Lake District using a Wright piston corer. In each site we obtained multiple cores from different microenvironments and selected the cores having the most complete, intact stratigraphy and highest sediment-accumulation rates. The palynological samples were processed following standard procedures and analyzed with a stereomicroscope at 400× magnification. The results are shown as percent abundance (for details (Moreno et al., 1999)). The identification of key stratigraphic sites shown in this study was done in the field after constructing detailed glacial geomorphologic maps and carrying out field surveys; each section was photographed, described and sampled carefully. We calculated weighted means for groups of replicate radiocarbon dates obtained in direct association with key stratigraphic sections and key palynological events. This enabled us to develop a radiocarbon framework for the LGM-LGT and millennial-scale changes embedded in their development. All radiocarbon dates are calibrated using the Intcal13 dataset and the OxCal 4.2 Program (Bronk Ramsey, 2009) (Supplementary Table 1). In the case of palynological records we developed Bayesian ages models using Bacon package for R (Blaauw and Christen, 2011) considering: (i) the density of radiocarbon dates through each record, with replicate dating for constraining the timing of specific events, (ii) the need for median age probability interpolates and (iii) the corresponding confidence intervals for each major transition in the pollen records.

## 4. Results

### 4.1. High-resolution pollen stratigraphy

We combined palynological records from Canal de la Puntilla (site 1 in Fig. 1) and Huelmo (site 2 in Fig. 1) in the lowlands of the Chilean Lake District (~150 m.a.s.l.) to examine the last transition from extreme glacial to extreme interglacial conditions, in view of their climate sensitivity, tight stratigraphic/chronologic control, high sediment-accumulation rates/sampling resolution, proximity (~80 km apart) and, most important, the common vegetation history in sections of the records that overlap in time (Hajdas et al., 2003; Moreno et al., 1999; Moreno and Leon, 2003). Both sites feature accumulation of organic-rich sediments in small closed basins that have similar depositional environments, are associated with glacial deposits/landforms dating to the LGM, and are located within the same vegetation and climate zones. Field and laboratory methods are described in detail by Moreno and Leon (2003).

The pollen record from Canal de la Puntilla (Fig. 2) integrates the palynology and radiocarbon chronology of cores 607AT2, 413BT1, and PM13 (Moreno et al., 1999), all of which exhibit overlapping segments that ensure stratigraphic continuity through the critical

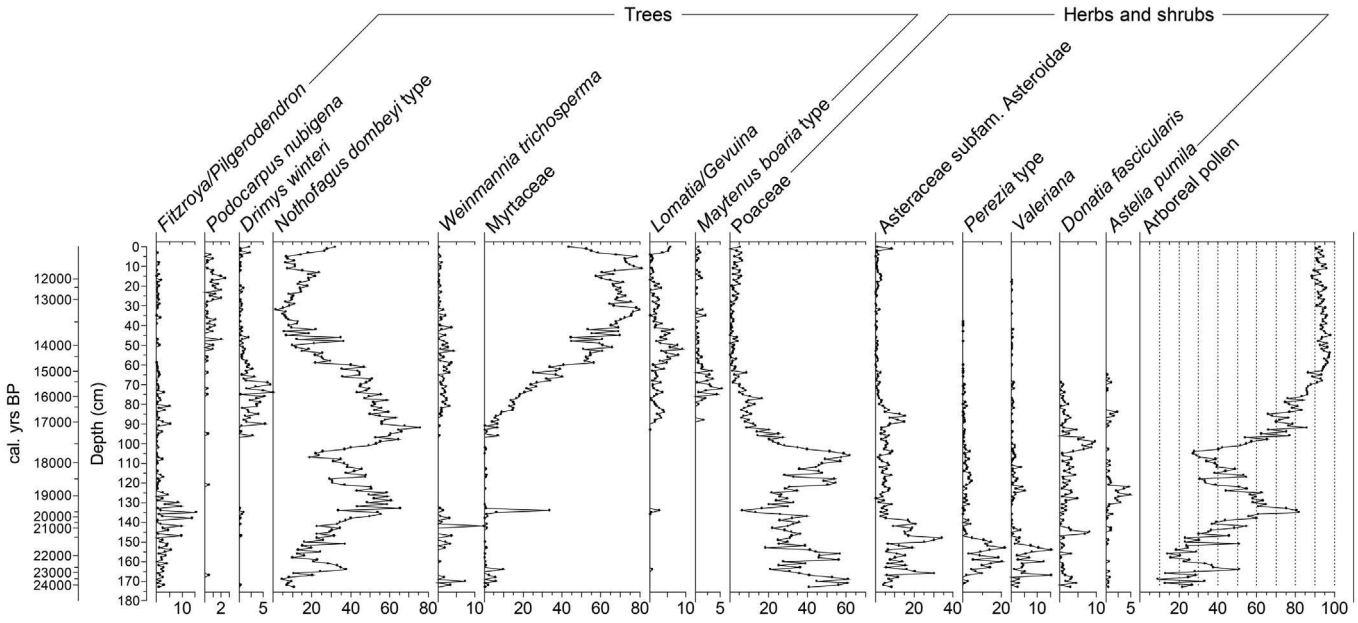


**Fig. 2.** Simplified pollen record from the Canal de la Puntilla site. This stacked record includes the pollen and radiocarbon data from cores 607AT2, 413BT1, and PM13. *Nothofagus* refers exclusively to the species included in the taxon *Nothofagus dombeyi* type. The red arrow indicates the maximum percentage values of *Nothofagus dombeyi* type (75.8% at 195 cm) with which we matched this record with the Huelmo pollen stratigraphy. The secondary y axis expresses the stacked age model.

interval encompassing the LGM-LGT and allow development of a new, statistically robust age model using the latest radiocarbon calibration datasets. This spliced record circumvents the heterogeneities related to slumps, thick wood layers, and associated hiatuses across different microenvironments within the site. Full details on the radiocarbon chronology, along with the sediment and high-resolution pollen stratigraphies for each core, are discussed in Moreno et al. (1999). A close match among high-resolution pollen records from the several cores from the Canal de la Puntilla site was achieved based on *Nothofagus dombeyi* type percentages of 43.4% and 42% at ~19,360 cal yrs BP (median probability age according to age model, 2σ confidence interval: 19,190–19,770 cal yrs BP) in cores 413BT1 and PM13, respectively, X-radiographs, loss on ignition (LOI), and high-resolution and replicate pollen stratigraphies on the overlapping zones, along with bracketing radiocarbon dates (minimum-limiting dates: AA-23254, AA-23252, maximum-limiting date: AA-9980) (Supplementary Table 1). We then adjusted the depths of pollen samples and radiocarbon dates from core PM13, and transferred additional radiocarbon ages from companion core PM12 to (i) bracket the chronology of a tephra with an interpolated median probability age of ~16,960 cal yrs BP according to the age model (2σ confidence

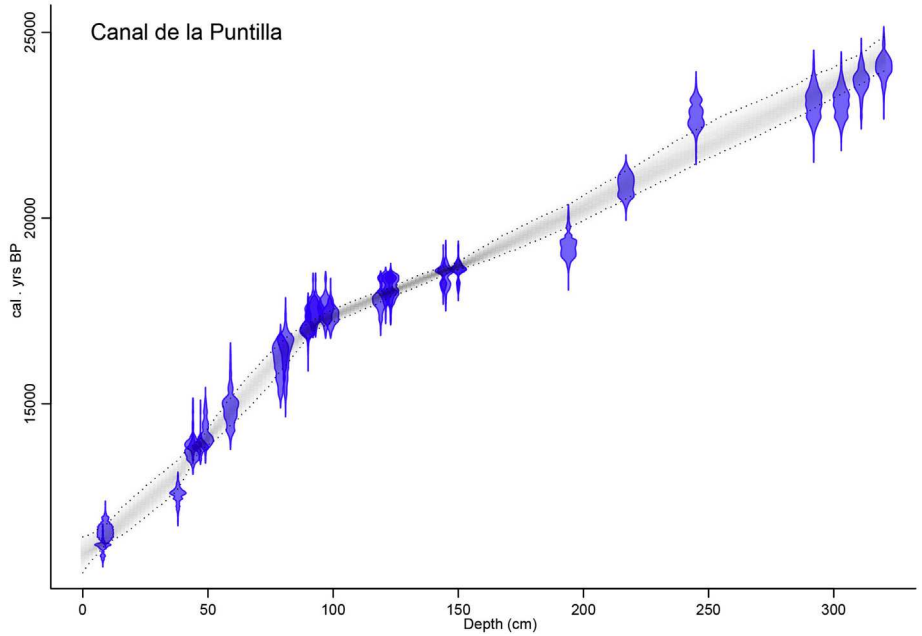


**Fig. 3.** Radiocarbon chronology and age model of the Canal de la Puntilla site. The x axis represents depths with no tephras, the y axis units are cal. yrs BP.

interval: 16,733–17,118 cal yrs BP), fully consistent with a close minimum-limiting radiocarbon date UGa-6987 and a close maximum-limiting radiocarbon date AA-23249 (Supplementary Table 1), (ii) provide close minimum-limiting dates for the deglacial *N. dombeyi* type rise (sequential dates AA-18253, AA-18255, AA-18256), and (iii) strengthen the chronology for the commencement of organic lacustrine sedimentation at the site (date Beta-80353). The chronology of the spliced record from Canal de la Puntilla is constrained by 31 radiocarbon dates (Supplementary Table 1), upon which we developed a Bayesian age model (Fig. 3) forced at 2-cm intervals, after subtracting the thickness of all tephras and wood layers in consideration of their instantaneous deposition. The entire Canal de la Puntilla pollen record spans the interval between 11,080 and 24,060 cal yrs BP according to the age model, with a median time step of 61 yr/cm between samples.

The pollen record from the Huelmo site (Figs. 1 and 4) was developed from overlapping cores 901B and 601A (Moreno and Leon, 2003). These cores were correlated with the aid of x-radiographs, LOI, magnetic susceptibility, radiocarbon dates (Supplementary Table 1), a tephra layer dated at ~ 11,000 cal yrs BP, and high-resolution and replicate pollen stratigraphies in the overlapping zone. The chronology of the Huelmo record is based on 36 radiocarbon dates (Supplementary Table 1), upon which we developed a Bayesian age model (Fig. 5), forced at 4-cm intervals, to assign interpolated ages to all levels analyzed, after subtracting the thickness of the 11,000 year-old tephra considering its instantaneous deposition. This age model suggests undisturbed, continuous, in-situ pelagic sedimentation, and high sediment accumulation rates between ~7450 and 18,950 cal yrs BP, with a median time resolution of 49 yr/cm between palynological samples.

To obtain a stacked record for the region, we spliced the pollen records from Canal de la Puntilla and Huelmo on the basis of the independently constrained chronology for the appearance and rapid increase of Myrtaceae, and peak percentages of *N. dombeyi* type that immediately preceded that expansion (Fig. 6). The precise match corresponds to the levels containing 75.8% (195 cm) and 74.1% (964 cm) abundance of *N. dombeyi* type in the Canal de la Puntilla and Huelmo records, respectively (Figs. 2 and 4). The age models interpolate median probability ages of 17,265 and 17,235 cal yrs BP (2σ confidence intervals: 17,170–17,610 and 17,047–17,377 cal yrs BP respectively) for peak *N. dombeyi* type abundance, respectively, consistent with the close limiting radiocarbon dates available from each site (Supplementary Table 1).

The stacked pollen record spans the interval between 7450 and 24,060 cal yrs BP with a median time resolution of 62 years between adjacent samples (Figs. 6 and 7). This record allows a detailed examination of the last transition from extreme-glacial to extreme-interglacial conditions along a time continuum. We calculated the rate-of-change parameter on the spliced pollen record to quantify the magnitude/rapidity of vegetation changes (Fig. 7). This was done by smoothing the pollen percentage data with a 5-point moving average, interpolating pollen samples at regular 150-year intervals, and calculating a dissimilarity coefficient (chord distance) per unit time between adjacent pollen levels (Moreno, 2004).

We now describe and give our interpretation of the stacked pollen record from Canal de Puntilla and Huelmo (Figs. 6 and 7). The pollen record between ~18,000 and 24,000 cal yrs BP shows abundant herbs (Poaceae, Asteraceae subfamily Asteroideae), high Andean herbs/shrubs (*Perezia* type, *Valeriana*), and cushion-bog species found today in Magellanic Moorland communities (*Astelia pumila*, *Donatia fascicularis*). Within this interval we detect an initial phase with the highest abundance of cold-resistant pioneer herbs and shrubs between ~23,400 and 24,000 cal yrs BP terminated by an increase from <10% to ~40% in cold-resistant hygrophilous subantarctic trees (*N. dombeyi* type, *Fitzroya/Pilgerodendron*) between ~ 22,600 and 23,400 cal yrs BP. This was followed by a reversal in trend that led to a peak in Poaceae between ~21,800 and 22,600 cal yrs BP, followed in turn by a resumption of the trend toward arboreal dominance that culminated with a peak of ~80% at 19,275 cal yrs BP (MAP = median probability age according to age model, 2σ confidence interval: 19,110–19,655 cal yrs BP), which we interpret as woodland encroachment in the lowlands of the Chilean Lake District. The trend culminated with a short-lived increase in Myrtaceae, a family of trees and shrubs whose regional abundance is highest at low-

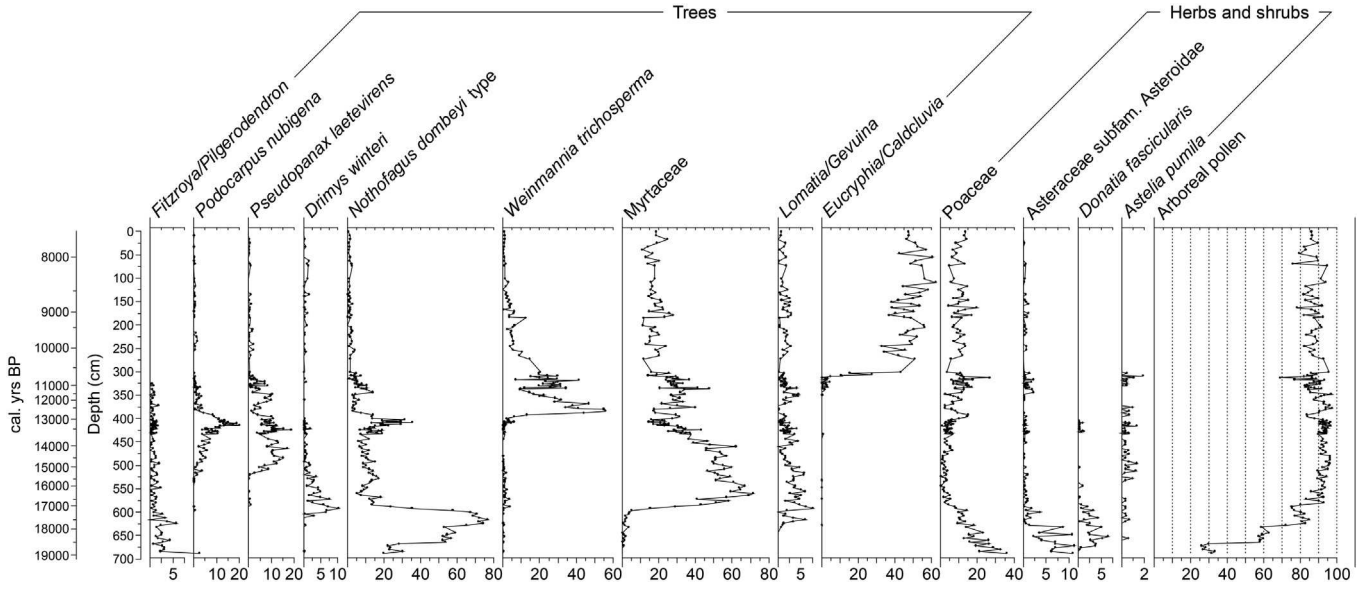


**Fig. 4.** Simplified pollen record from the Huelmo site. This stacked record includes the pollen and radiocarbon data from cores 601A and 9901A. *Podocarpus* refers exclusively to the species *P. nubigena*, the *Eucryphia/Caldcluvia* palynomorph includes the trees *Eucryphia cordifolia* and *Caldcluvia paniculata*. The red arrow indicates the maximum percentage values of *Nothofagus dombeyi* type (74.1% at 964 cm) with which we matched this record to the Canal de la Puntilla pollen stratigraphy.

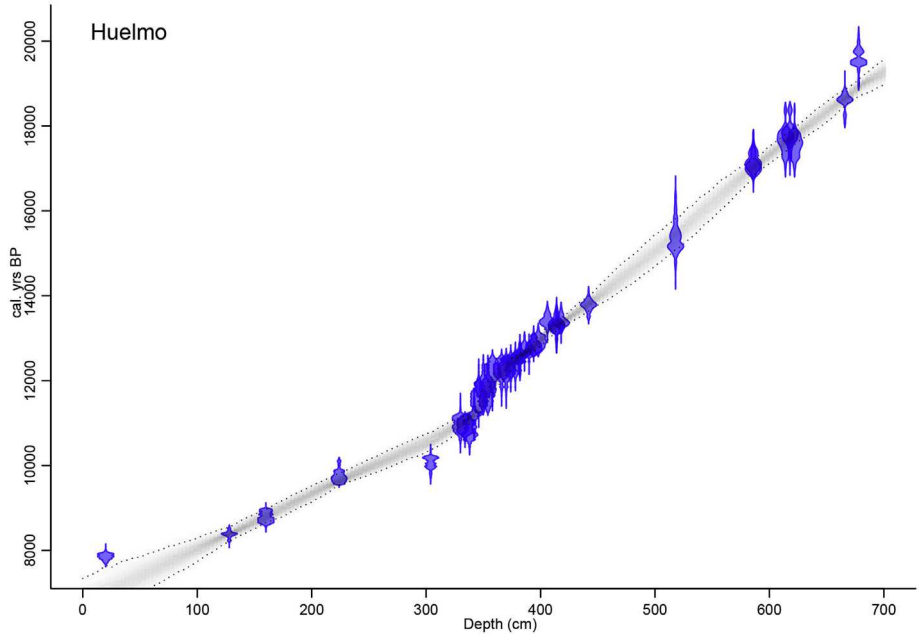


**Fig. 5.** Radiocarbon chronology and age model of the Huelmo site. The x axis represents depths with tephras removed, the y axis units are cal. yrs BP.

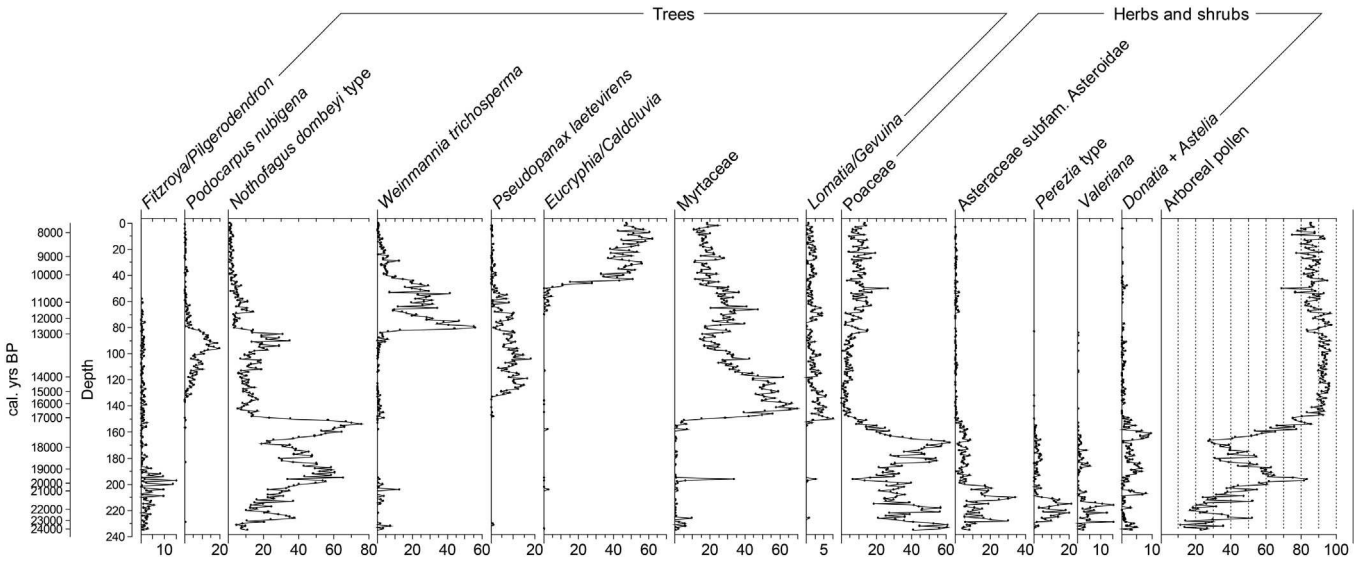


**Fig. 6.** Stacked pollen record from Canal de la Puntilla and Huelmo. The primary y axis shows the depth scale, the secondary y axis presents the spliced age scale. The variables selected depict variations in the composition of the vegetation ranging from an open landscape dominated by herbs and shrubs to closed-canopy rainforests.

and mid-elevation North Patagonian rainforest communities. These data suggest an initial pioneer phase with a sparsely vegetated landscape dominated by cold-resistant hygrophilous herbs with near absence of arboreal pollen (<10%), suggesting that the lowlands of northwestern Patagonia harboured scattered low-density tree populations in a vegetation matrix composed by species characteristic of modern high-Andean environments and Magellanic Moorland communities during the LGM. These results and interpretations suggest extreme cold and wet conditions with an inferred depression of ~1000 m in the regional treeline relative to modern conditions between ~23,400 and 24,000 and between ~21,800 and 22,600 cal yrs BP, in agreement with previous studies (Heusser et al., 1999, 1996b). Our results indicate that moderate and gradual warming within the LGM, drove a transition from an open landscape dominated by alpine herbs to open *Nothofagus* forests interspersed with Magellanic Moorland communities, overprinted by a reversal between ~21,800 and 22,600 cal yrs BP. The sustained increase in arboreal abundance culminated with a brief incursion of thermophilous trees/shrubs at ~19,300 cal yrs BP. These vegetation changes are best explained by a gradual and sustained rise in the regional treeline in response to warmer conditions between ~19,300 and 23,400 cal yrs BP.

A reversal in the trend toward arboreal dominance occurred between ~17,800 and 19,300 cal yrs BP, marked by an abrupt decline in arboreal pollen from ~80% to ~30% and an increase in grass pollen, as well as high Andean/Subantarctic and Magellanic Moorland taxa (Figs. 6 and 7). The onset of this trend is constrained by a maximum-limiting AMS age of 16,085 ± 220 $^{14}$C yrs BP

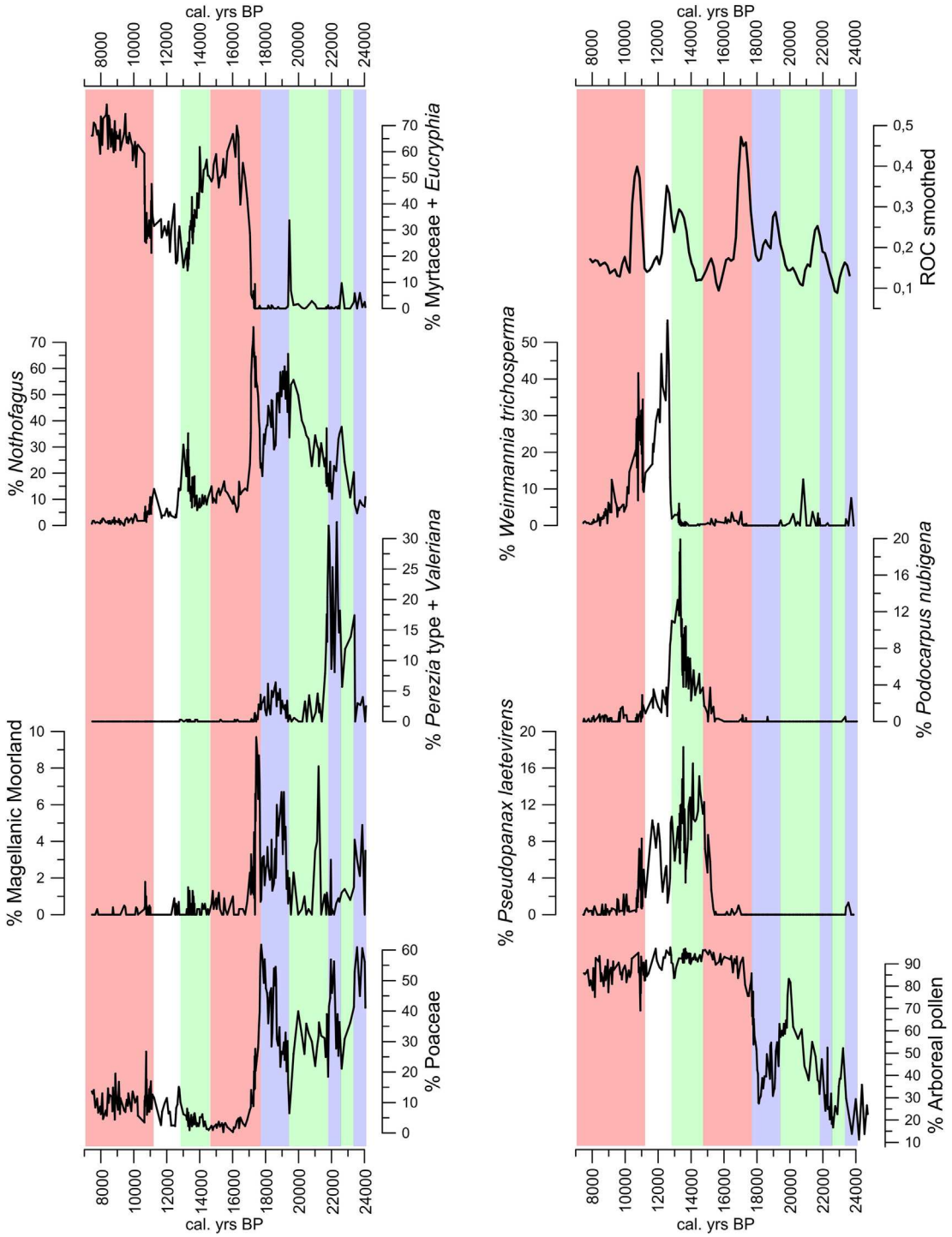


**Fig. 7.** Selected taxa from the stacked pollen record from Canal de la Puntilla and Huelmo sites along with results of the rates-of-change (ROC) calculation expressed in age scale. The calculation of ROC was performed on all terrestrial taxa from the stacked record having abundances >2%. The vertical blue bars represent extreme glacial conditions, green bars represent cold-temperate conditions, red bars represent warm conditions, see text for discussion on the interpretation of the pollen record. The portion of the record dated between ~11,000 and 13,000 cal yrs BP, shown without color, corresponds to an interval of intense fire activity and disturbance of the rainforest vegetation under cold-temperate conditions and a highly variable precipitation regime. (For interpretation of the references to colour in this figure legend, the reader is referred to the web version of this article.)

(19,417 ± 273 cal yrs BP) (Supplementary Table 1) and a cluster of close minimum-limiting ages with a weighted mean of 15,355 ± 52 $^{14}$C yrs BP (cluster E, 18,633 ± 68 cal yrs BP) (Supplementary Table 2). We interpret these palynological changes as an abrupt onset of cold and hyperhumid conditions, most likely driven by a lowering of the regional treeline and a stronger influence of the southern westerly winds. These changes led to the reestablishment of extreme glacial conditions between ~17,900 and 19,300 cal yrs BP.

A rapid increase of *N. dombeyi* type at 17,730 cal yrs BP (MAP, 2σ confidence interval: 17,677–17,982 cal yrs BP) marked the commencement of the LGT (Figs. 6 and 7), accompanied by a short-

lived increase in Magellanic Moorland taxa and a massive decline in all herbs and shrubs. The genus *Nothofagus* includes opportunistic pioneer species that commonly dominate the early stages of forest colonization of disturbed surfaces and newly deglaciated terrain (Veblen et al., 1996). Therefore, we infer that the *N. dombeyi* type rise represents an immediate response of the local vegetation to a warm pulse that ended LGM conditions and initiated the LGT. We note that Magellanic Moorland declined and virtually disappeared within a few hundred years after the initiation of the LGT (MAP: 17,298 cal yrs BP, 2σ confidence interval: 17,055–17,405 cal yrs BP), an aspect we interpret as a shift from hyperhumid conditions during the LGM to a less humid interval. This transition is best explained by a poleward displacement of the southern westerly wind belt with the onset of the LGT (Denton et al., 1999a; Moreno et al., 1999, 2012; Pesce and Moreno, 2014). The beginning of the LGT is bracketed by a cluster of maximum-limiting ages from a narrow stratigraphic interval having a weighted mean of 14,794 ± 55 $^{14}$C yrs BP (cluster D, 17,997 ± 89 cal yrs BP) (Supplementary Table 2), and a cluster of close minimum-limiting ages with a weighted mean of 14,538 ± 65 $^{14}$C yrs BP (cluster C, 17,720 ± 105 cal yrs BP) (Supplementary Table 2). We interpret the rapid increase in *N. dombeyi* type and the irreversible disappearance of cryophilic/hygrophytic herbs at ~17,800 cal yrs BP (age estimate based on bracketing clusters C and D) of dates as an abrupt rise in the regional treeline in response to warming at the beginning of the LGT, which drove alpine environments upslope from the lowlands of northwestern Patagonia and permitted the development of continuous lowland *Nothofagus* forest cover.

Thermophilous North Patagonian rainforest taxa (Myrtaceae, Proteaceae, *Drimys*, *Weinmannia*, *Hydrangea*, *Pseudopanax*, *Escallonia*, *Maytenus*) then increased abruptly at 17,100 cal yrs BP (MAP, 2σ confidence interval: 17,328–16,943 cal yrs BP) as *N. dombeyi* type and high Andean/Subantarctic taxa plummeted to minimum values (Figs. 6 and 7). The timing of this event is bracketed by a cluster of close maximum-limiting ages having a weighted mean of 14,377 ± 57 $^{14}$C yrs BP (cluster B, 17,522 ± 102 cal yrs BP) (Supplementary Table 2), and a cluster of close minimum-limiting ages with a weighted mean of 14,014 ± 43 $^{14}$C yrs BP (cluster A, weighted mean: 17,018 ± 119 cal yrs BP) (Supplementary Table 2). We interpret this vegetation turnover as an acceleration/intensification of the warm pulse that initiated the LGT at ~17,800 cal yrs BP.

Our results indicate that species-rich closed-canopy North Patagonian rainforests dominated by thermophilous trees, vines (arboreal pollen >90%) and epiphytic ferns were fully established in the lowlands by ~16,800 cal yrs BP, suggesting that climate and vegetation reached temperate-humid conditions within ~1000 years after the warm pulse that initiated the LGT (Figs. 6 and 7). Maximum-limiting ages for the onset of this change are afforded by Cluster A of dates (Supplementary Table 2).

A ~2000-ýear long interval ensued with dominance of shade-tolerant warmth-demanding North Patagonian trees. This interval was terminated by rises in *Podocarpus nubigena* and *Pseudopanax laetevirens* along with a reexpansion of *N. dombeyi* type, signaling a shift toward a North Patagonian rainforest community with cold-resistant hygrophilous conifers. These changes suggest that increased precipitation of westerly origin and a moderate lowering of the regional treeline drove a downward shift of montane forests under cooler and wetter climate. The onset of this change is bracketed by a minimum-limiting age of 11,930 ± 75 $^{14}$C yrs BP (13,766 ± 114 cal yrs BP) and a maximum-limiting age of 12,825 ± 80 $^{14}$C yrs BP (15,315 ± 141 cal yrs BP) (Supplementary Table 1). The age model interpolates an age of 14,722 cal yrs BP (MAP, 2σ confidence interval: 14,528–15,258 cal yrs BP) for the onset of this cold reversal. *N. dombeyi* type, *Podocarpus nubigena* and *P. laetevirens* increased rapidly until they reached peak abundance at 13,010 cal yrs BP (MAP, 2σ confidence interval: 12,866–13,161 cal yrs BP), according to the age model. This interpolated age is substantiated by a close maximum-limiting age of 11,550 ± 90 $^{14}$C yrs BP (13,382 ± 87 cal yrs BP) and a close minimum-limiting age of 11,040 ± 85 $^{14}$C yrs BP (12,905 ± 90 cal yrs BP) (Supplementary Table 1).

*N. dombeyi* type, *Podocarpus nubigena, and P. laetevirens* then declined as *Weinmannia trichosperma* and charcoal rose to peak abundance in a rapid vegetation change between ~12,000 and 13,000 cal yrs BP (Figs. 6 and 7). These changes were followed by vegetation recovery with modest increases in Myrtaceae and Poaceae pollen (most likely bamboo species of the genus *Chusquea*), and further declines in *N. dombeyi* type and *Podocarpus nubigena* and all other taxa. The magnitude, rapidity and palynological character of this change suggest disruption of temperate rainforest dominance by paleofires and proliferation of fast-growth, shade-intolerant herbs and cold-resistant North Patagonian trees favored by disturbance (Abarzua and Moreno, 2008; Jara and Moreno, 2012; Moreno et al., 2001; Moreno and Leon, 2003) between ~ 12,000 and 13,000 and between ~ 10,700 and 11,100 cal yrs BP. Fire activity in the broad-leaved evergreen temperate rainforest region of western Patagonia is highly dependent upon recurrent droughts, considering that fuel loads are not a limiting factor (Holz and Veblen, 2012), implying high variability in precipitation regime and/or enhanced rainfall seasonality over the ~11,000–13,000 cal yrs BP interval, which has recently been interpreted as a southward shift of the southern westerly winds during the LGT (Moreno et al., 2012; Pesce and Moreno, 2014).

Finally, we observe an abrupt increase in the thermophilous, summer-drought resistant tree *Eucryphia/Caldcluvia* at 10,750 cal yrs BP (MAP, 2σ confidence interval: 10,497–10,917 cal yrs BP), defining a multi-millennial phase with dominance of Valdivian rainforest that lasted until ~7500 cal yrs BP (Fig. 6). This upland vegetation change was contemporaneous with a lake regressive phase that led to terrestrialization of the Huelmo lake and the highest accumulation rates of charcoal (Moreno and Leon, 2003). These results indicate peak warmth and the lowest amount of precipitation in the record, suggesting peak interglacial conditions brought by weak westerly wind circulation at continental and zonal scale (Fletcher and Moreno, 2012; Moreno et al., 2010; Pesce and Moreno, 2014; Villa-Martinez et al., 2012).

Palynological records from Lago Condorito (Moreno, 2004) (site LC in Fig. 1) and Lago Lepué (Pesce and Moreno, 2014) (site 33 in Fig. 1), located in the lowlands of the Chilean Lake District and Isla Grande de Chiloé respectively, show multi-millennial alternations between thermophilous Valdivian rainforests resistant to summer moisture stress and North Patagonian rainforests with cold-resistant hygrophilous conifers over the last ~ 16,000 years. Moreno (2004) developed a standardized palynological index that combines the diagnostic species from these rainforest communities as end members of the total range of temperate rainforest and climate variability in the region over the last ~ 16,000 years. The interval between ~14,600 and 16,000 cal yrs BP in the Lago Condorito and Lepué records features a conspicuous assemblage with species common to both rainforest communities but lacking those key indicator species of the Valdivian and North Patagonian rainforest, thus defining index values approaching zero that correspond to the average of the last ~16,000 years. The pollen records from Canal de la Puntilla and Huelmo show that this average condition prevailed between ~14,700 and 16,700 cal yrs BP in the context of a landscape dominated by dense, closed-canopy rainforests (arboreal pollen > 90%), with the implication that vegetation and climate over this interval represent average interglacial conditions in the lowlands of northwestern Patagonia. Hence, the warm pulses at ~17,800 and ~17,100 cal yrs BP brought extreme glacial climate to

average Holocene values within ~1000 years. The rates-of-change parameter (Fig. 7) reveals that this transition was extraordinarily rapid. The abruptness of this change is similar (but larger) to the onset of peak Holocene warmth and substantial decline in precipitation between 10,000 and 11,000 cal yrs BP. Because North Patagonian rainforests lacking cold-resistant conifers currently occur at mid-elevations (lower altitudinal limit: 350 ± 100 m.a.s.l.) in the mountain ranges of the Chilean Lake District at 41°S, and the modern treeline is located at 1100 ± 100 m.a.s.l. at the same latitude, we estimate that the shift from High Andean grassland/scrubland to closed-canopy North Patagonian rainforests at the onset of the LGT is best explained by a treeline rise of ~750 m, i.e. about 75% the total amount of treeline lowering during the LGM. Rapid changes of lower magnitude are evident during cold reversals at ~22,000, ~19,000 and ~14,000 cal yrs BP and at the onset of a cold interval with highly variable precipitation regime and intense fire activity that began at ~13,000 cal yrs BP. Warm events at the beginning of the Holocene account for the remaining 25% rise in the regional treeline rise, leading to an extreme warm/dry multimillennial phase between 7500 and 10,750 cal yrs BP.

### 4.2. Glacial morphology, stratigraphy and geochronology

To place the glacial-geomorphology record of the LGT in context, we first present the timing of expansion of Andean ice lobes into the Llanquihue (LGM) moraine belt in the Chilean Lake District and on Isla Grande de Chiloé. We then present the chronologic data that confine the collapse of these ice lobes from the Llanquihue moraine belt back into the Andes during the LGT.

Fig. 1 depicts the configuration of Andean piedmont ice lobes in the Chilean Lake District and on Isla Grande de Chiloe during maximum phases of the last glaciation, locally referred to as the Llanquihue glaciation. This reconstruction is based largely on glacial morphologic mapping of Llanquihue moraines (depicted schematically in red (in the web version) in Fig. 1) and outwash plains near lakes and marine water bodies alongside the western margin of the Andes. Detailed glacial geomorphological maps given in Andersen et al. (1999) and Denton et al. (1999b) illustrate not only Llanquihue moraines and outwash plains, but also display the older Casma and Colegual moraines and outwash plains first described by Mercer (1976). Where applicable, radiocarbon dating of Llanquihue landforms shows that Andean ice lobes advanced into the moraine belt depicted in red (in the web version) in Fig. 1, and hence achieved glacial maxima, numerous times during MIS 4, MIS 3, and MIS 2, rather than simply during the time of the global LGM in MIS 2 (Clark et al., 2009). A notable example occurs on Isla Grande de Chiloé. Here the radiocarbon chronology and vegetation history of a core from the Taiquemó mire indicate that the outermost Llanquihue-age ridge considerably antedates the global LGM, and was probably deposited during MIS 4 (Heusser et al., 1999).

The chronology for expansion of Andean piedmont glacier lobes into Llanquihue-age moraine belts comes from radiocarbon dates at several key stratigraphic sections (Denton et al., 1999b). First, at site 3 in Fig. 1 at the top of an ice-contact slope that rises high above Bahía Octay of Lago Llanquihue, an outwash unit rests on organic-rich pyroclastic deposits. The topographic position of the outwash requires that the source of the meltwater must have been a glacier lobe that terminated at the upper crest of the ice-contact slope (Denton et al., 1999b). As listed in Supplementary Tables 2 and 3, radiocarbon dates of five organic samples collected from the upper surface of the pyroclastic flow deposit, sealed by outwash sediments, afford a mean value of 29,384 ± 176 $^{14}$C yrs BP (33,594 ± 187 cal yrs BP). Second, at site 4 in Fig. 1, flow till rests on an intact former land surface developed on pyroclastic flow sediments. The site lies near the top of the lakeside ice-contact slope (Denton et al., 1999b). The ice lobe responsible for the overlying flow till that sealed this surface extended at least to the top of this ice-contact slope, which is located within 6 km of the outermost Llanquihue-age moraine. Seventeen radiocarbon dates of wood and organic-rich pyroclastic flow sediments, listed in Supplementary Table 3, yielded a mean of 26,550 ± 85 $^{14}$C yrs BP (30,823 ± 99 cal yrs BP, Supplementary Table 2). Third, at site 5 in Fig. 1, alongside Seno Reloncaví, wood and fibrous peat from the upper surface of an organic bed is sealed by outwash that, in turn, is overlain by Llanquihue-age moraines (Denton et al., 1999b). The meltwater responsible for the outwash emanated from an ice lobe that reached to the top of the ice-contact slope high above Seno Reloncaví. The ice lobe subsequently advanced over the outwash deposit. As listed in Supplementary Tables 2 and 3, radiocarbon dates of four samples from the organic horizon give a mean age of 22,566 ± 86 $^{14}$C yrs BP (26,887 ± 168 cal yrs BP) (Supplementary Table 2) for burial by this outwash (Denton et al., 1999b). Fourth, at the Teguaco site (site 6 in Fig. 1) on Isla Grande de Chiloé, organic litter from the upper surface of a gyttja layer is sealed intact beneath glaciolacustrine silt and clay (Denton et al., 1999b). The local topography indicates deposition of these lacustrine sediments in a lake dammed by the Golfo de Corcovado ice lobe when it advanced onto the eastern flank of Isla Grande de Chiloé. Radiocarbon dates of twelve samples from the organic litter, listed in Supplementary Table 3, afford a mean age of 22,464 ± 47 $^{14}$C yrs BP (26,787 ± 150 cal yrs BP) (Supplementary Table 2) for flooding by the ice-dammed lake (Denton et al., 1999b). Finally, site 7 in Fig. 1, first reported here, features a section in Llanquihue drift that was revealed as Route 5 was being expanded in 2001 in the western sector of Puerto Montt. This section reveals glacial sediments resting on a pyroclastic flow deposit(s) (Fig. 8). The organic litter of the old ground surface on the pyroclastic deposit is preserved intact beneath overlying gravelly diamicton, with a thin cap of lodgment till, which extends unbroken to the present-day surface ground moraine. The faintly bedded diamicton is interpreted as gravelly sediment flows from a former ice margin onto the adjacent land surface, protecting its soil-and-organic cover. The banded appearance of the diamicton comes from the stacking of several individual sediment flows. Because it contains numerous round-to-semiround clasts, the flow material probably was sourced from outwash terraces and moraine cores and incorporated into overriding ice. Radiocarbon ages of four small pieces of wood from the organic litter on the buried land surface afford a mean age of 21,789 ± 44 $^{14}$C yrs BP (26,007 ± 66 cal yrs BP) (Supplementary Tables 2 and 3), thus dating an advance over the site of the Seno Reloncaví ice lobe.

Two sets of radiocarbon dates afford bracketing ages for the Llanquihue moraine belt outboard (west) of Lago Llanquihue (Denton et al., 1999). One set affords maximum-limiting ages derived from organic clasts reworked into outwash graded to the outer moraine ridges. Site 8 in Fig. 1 afforded a clast age of 23,020 ± 280 $^{14}$C yrs BP (27,280 ± 268 cal yrs BP). Site 9 yielded a clast age of 20,840 ± 400 $^{14}$C yrs BP (25,060 ± 457 cal yrs BP) (Supplementary Table 3). Site 10 afforded a clast age 25,100 ± 420 $^{14}$C yrs BP (29,259 ± 501 cal yrs BP) (Supplementary Table 2). Site 11 near Frutillar Alto yielded clast ages as young as 21,840 ± 700 $^{14}$C yrs BP (26,195 ± 728 cal yrs BP), 22,790 ± 410 $^{14}$C yrs BP (27,019 ± 400 cal yrs BP), 21,120 ± 180 $^{14}$C yrs BP (25,540 ± 201 cal yrs BP), and 22,700 + 180/−175 $^{14}$C yrs BP (27,004 ± 230 cal yrs BP) (Supplementary Table 3). The second set of radiocarbon dates affords minimum-limiting ages for the Llanquihue moraine belt fronting Lago Llanquihue. The ice had abandoned these moraines and had retreated back to the lakeside ice-contact slope by 20,160–20,580 $^{14}$C yrs BP (24,220–24,770 cal yrs BP), as shown by ages from the base of organic-rich fills in Canal de la Puntilla (site 1 in Fig. 1) and Canal de Chanchán (site 12 in Fig. 1).

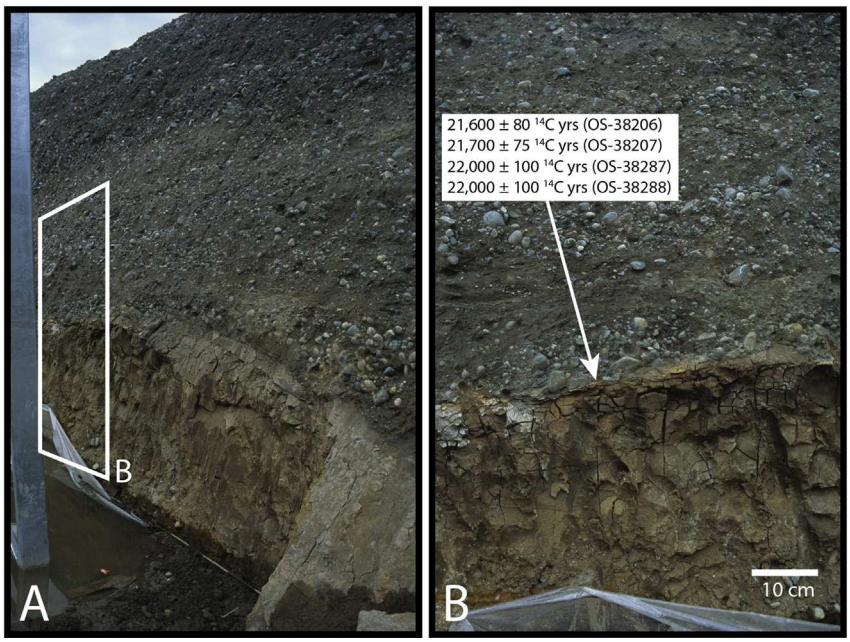


**Fig. 8.** Photographs with vantage eastward of the stratigraphic section at site revealed on the east side of Route 5 during widening in 2001. As described in the text a gravelly diamicton rests on sediments of a pyroclastic flow. The old land surface is preserved intact on the pyroclastic flow deposits. The position and age of dated wood samples from this surface are shown. The interpretation of the section and ages appear in the text.

Another minimum-limiting age near the lakeside ice-contact slope is 19,760 + 250/−240 $^{14}$C yrs BP (23,788 ± 305 cal yrs BP) from site 13 in Fig. 1. Minimum-limiting ages for outer Llanquihue moraines are 19,993 ± 256 $^{14}$C yr BP (24,072 ± 325 cal yrs BP) from Fundo Línea Pantanosa at site 14 in Fig. 1, and 20,680 ± 175 $^{14}$C yrs BP (24,900 ± 258 cal yrs BP) from Fundo Llanquihue at site 15 in Fig. 1.

Of particular importance to the chronology of the LGT is the timing of the youngest advance of Andean ice lobes into the Llanquihue moraine belts of Fig. 1. Chronological data for this event are available from sites tied to the former Llanquihue, Reloncaví, Ancud, and Golfo de Corcovado ice lobes (Denton et al., 1999b). We discuss the pertinent sites from north to south. During this most recent advance, a large piedmont ice lobe filled the basin of Lago Llanquihue and reached to the innermost ice-contact slope of the Llanquihue moraine belt along the western margin of the lake. Here meltwater from the lobe deposited an extensive kame terrace that was banked against the lakeside ice-contact slope on its outboard side and supported by the ice lobe on its inboard side. At several localities on the western margin of Lago Llanquihue, the lacustrine and alluvial sediments that make up this kame terrace rest conformably on, and seal off, the intact upper surface of organic deposits assigned by Mercer (1972) to the Varas Interstade. Radiocarbon dates of organic samples from this upper surface thus constrain the culmination of an advance of the Llanquihue ice lobe to the western margin of the lake. At the Llanquihue site (18 in Fig. 1), seven such samples yielded a mean age of 14,824 ± 42 $^{14}$C yrs BP (18,026 ± 81 cal yrs BP) (Supplementary Tables 2 and 3). In addition, radiocarbon dates of samples from the upper surface of intact peat at four sites in the Puerto Varas embayment mark deposition of kame sediments. At the Northwest Bluff site (site 19 in Fig. 1), two samples yielded a mean age of 14,883 ± 72 $^{14}$C yrs BP (18,099 ± 107 cal yrs BP) (Supplementary Tables 2 and 3). At the Calle Santa Rosa site (20 in Fig. 1), a single sample gave an age of 14,820 ± 230 $^{14}$C yrs BP (18,040 ± 272 cal yrs BP). At the railroad bridge site (16 in Fig. 1), seven samples afforded a mean age of 14,512 ± 30 $^{14}$C yrs BP (17,694 ± 87 cal yrs BP) (Supplementary Tables 2 and 3). Finally, at the Bella Vista bluff section (site 17 in Fig. 1), seven samples provided a mean age of 14,610 ± 32 $^{14}$C yrs BP (17,795 ± 82 cal yrs BP) (Supplementary Tables 2 and 3).

A radiocarbon date of 15,220 ± 80 $^{14}$C yrs BP (18,485 ± 102 cal yrs BP) affords a close maximum-limiting age for advance of the Reloncaví ice lobe over site 21 in Fig. 1, located on Isla Maillén (Supplementary Table 3). Radiocarbon dates of four samples collected from a stratigraphic section at the Punta Penas section, site 24 in Fig. 1, register this advance onto the ice-contact slope at 14,882 ± 42 $^{14}$C yrs BP (18,088 ± 87 cal yrs BP). Radiocarbon dates of organic clasts reworked into outwash at sites 22 and 23 in Fig. 1 indicate that this advance culminated shortly after 15,000 $^{14}$C yrs BP (18,220 cal yrs BP), when it reached to the top of the high ice-contact slope at the inboard flank of the Llanquihue moraine belt on the western margin of Seno Reloncaví. The ages of peat clasts at sites 22 and 23 in Fig. 1 (Supplementary Table 3), reworked into outwash, graded to the upper lip of the ice-contact slope, along with the age of basal organic material from the Huelmo mire (site 2 in Fig. 1), show that ice of this advance did not push far into the Llanquihue moraine belt west of Seno Reloncaví.

The Golfo de Ancud piedmont ice lobe, located south of Seno Reloncaví, underwent an extensive advance shortly after 15,000 $^{14}$C yrs BP (18,300 cal yrs BP) that reached to within 4 km of the outer limit of the Llanquihue moraine belt (Denton et al., 1999b). The radiocarbon dates at site 25 in Fig. 1 are important for this conclusion. Here, drift deposited during this advance features numerous reworked peat clasts, ten of which yielded radiocarbon dates ranging from 15,730 ± 70 $^{14}$C yrs BP (18,900 ± 150 cal yrs BP) to 14,900 ± 155 $^{14}$C yr BP (18,180 ± 230 cal yrs BP) (Supplementary Table 3). Each of these dates affords a maximum-limiting value for deposition of the drift. Widespread fluting on the drift surface suggests that ice advancing from the southeast overran the site and reached close to the outer limit of Llanquihue moraines.

The northern sector of the Golfo de Corcovado piedmont glacier underwent a strong advance onto Isla Grande de Chiloé shortly after 15,000 $^{14}$C yrs BP (18,300 cal yrs BP) (Denton et al., 1999). Ice of this advance deposited outwash on, and then overrode, an organic bed at Dalcahue (site 26 in Fig. 1). The ice front pushed forward at

least to the next moraine ridge a few hundred meters outboard of the Dalcahue site (Denton et al., 1999b). The intact surface of the overridden organic bed at Dalcahue yielded 32 radiocarbon dates (Supplementary Table 3), which gave a mean value of 14,780 ± 20 $^{14}$C yrs BP (18,035 ± 215 cal yrs BP) (Supplementary Table 2). That this advance over the Dalcahue site was the most extensive of MIS 2 is shown by 20 radiocarbon dates of closely spaced samples taken in vertical succession from just below the surface (18,445 ± 140 $^{14}$C yrs BP; 21,970 ± 230 cal yrs BP) to the base of the organic bed (30,070 ± 220 $^{14}$C yrs BP; 34,740 ± 180 cal yrs BP).

Overall, the glacial geomorphological mapping and the associated chronological data show an increase in the extent of the advance shortly after 15,000 $^{14}$C yrs BP (18,300 cal yrs BP) between the Llanquihue and Reloncaví piedmont lobes to the north, and the Ancud and the Corcovado lobes to the south. In the two northern lobes the advance reached only to the inner margin of the LGM moraine belt, whereas the advance of the two southern lobes was either the most extensive, or else close to the most extensive, of MIS 2.

Several radiocarbon dates afford minimum-limiting values for recession from the outer limit achieved by piedmont ice lobes during the widespread advance that culminated shortly after ~15,000 $^{14}$C yrs BP (~18,300 cal yrs BP). Lowell et al. (1995) and Denton et al. (1999b) reported basal radiocarbon dates from sediment cores retrieved from mires located on moraine belts fringing Lago Llanquihue, Seno Reloncaví, and Isla Grande de Chiloé. Most of those dates constitute minimum-limiting ages for glacial landforms that precede the final advance into the Llanquihue moraine belt, except for those from three sites located in the central-east portion of Isla Grande de Chiloé. These sites are the Mayol (site 27 in Fig. 1), Estero Huitanque (site 28 in Fig. 1; Heusser et al., 1999) and unnamed bogs (site 29 in Fig. 1) that yielded basal ages of 14,940 ± 100 $^{14}$C yrs BP (18,164 ± 129 cal yrs BP), 13,345 ± 105 $^{14}$C yrs BP (16,050 ± 155 cal yrs BP), and 13,560 ± 95 $^{14}$C yrs BP (16,351 ± 156 cal yrs BP), respectively (Lowell et al., 1995) (Supplementary Table 3). These sites are located near the eastern coast of Isla Grande de Chiloé on morainal deposits from the final advance of the Golfo de Corcovado ice lobe into the Llanquihue moraine belt. Additional dates of 14,050 ± 80 $^{14}$C yrs BP (17,076 ± 152 cal yrs BP) and 13,820 ± 90 $^{14}$C yrs BP (16,722 ± 166 cal yrs BP) have recently been reported from near-basal organic samples in piston cores from the deepest sectors of Lago Tahui (30 in Fig. 1) and Lago Melli (31 in Fig. 1) (Abarzua and Moreno, 2008), situated ~ 30 km southeast of the Mayol and Estero Huitanque sites (Supplementary Table 3). The spread of ~2000 years in the basal dates from these Chilotan mires and lacustrine sediments, all of which are minimum-limiting values for deglaciation, can be attributed in part to differences in dating (conventional vs. AMS) and in sampling techniques (piston corer vs. Hiller or Dachnovsky borer), as well as site types (mire vs. shallow or deep sector of a closed-basin lake) and local paleohydrology. This spread motivated us to obtain additional basal ages from pertinent sites to constrain more precisely the chronology of recession from the outer position of the final Llanquihue advance. For that purpose we obtained AMS radiocarbon dates of the basal organic levels from the most complete stratigraphies revealed by sediment cores along a bathymetric transect at each site, retrieved using a Wright square piston corer from an anchored platform. We selected small, closed-basin lakes having at least 6 m of water depth, located in depressions on morainal topography associated with the final Llanquihue advance of the Rupanco, Reloncaví, and Corcovado ice lobes. We now discuss these new dates, along with the most pertinent of the dates obtained previously.

Organic matter from the base of cores through lacustrine sediments accumulated in morainal basins on Isla Grande de Chiloé inboard of the limit of this youngest advance of the Corcovado ice lobe comes from two particularly important sites. One of them is located in the foothills of Cordillera de la Costa, 25 km west of the eastern coast. The other is situated near the eastern coast of Chiloe in an inter-moraine depression. These morainal sediments were deposited by the Golfo de Corcovado ice lobe during the advance that overrode the Dalcahue organic bed. The first locality is Lago Tarumán (site 32 in Fig. 1). Here we obtained multiple overlapping sediment cores using a square-rod Livingstone piston corer from a platform anchored on the deepest part of the lake. Gyttja from a depth of 806 cm in an 828-cm-long core to the base of the lacustrine sediments yielded an age of 14,175 ± 40 $^{14}$C yrs BP (17,263 ± 96 cal yrs BP), consistent with several dates in stratigraphic order higher in the core (Gonzalorena, 2015) (Supplementary Table 3). At the second site, Lago Lepué (site 33 in Fig. 1), we collected overlapping piston cores of lacustrine sediments from different depositional environments along a bathymetric transect and obtained a series of radiocarbon dates throughout the core stratigraphies. Replicate dates from the base of 1200-cm long cores retrieved from the deepest sector of the lake yielded nearly identical values of 14,700 ± 90 and 14,700 ± 95 $^{14}$C yrs BP (combined calendar age is 17,886 ± 120 cal yrs BP) (Supplementary Table 2) (Pesce and Moreno, 2014), also supported by additional dates in stratigraphic order higher in the core stratigraphy. Taken together, the dates from Lago Tarumán, Lago Lepué, and Mayol imply that by 14,780 $^{14}$C yrs BP (~17,800 cal yrs BP) the Golfo de Corcovado ice lobe had retreated well inboard of the eastern slopes of Cordillera de la Costa and the outer Llanquihue limit achieved by ice that overran the Dalcahue organic bed. An additional implication is that the maximum of the advance of the Golfo de Corcovado piedmont glacier over the Dalcahue site was short-lived, as the age of the top of the organic bed at Dalcahue is nearly identical to the minimum-limiting dates of ice recession from the sites at Mayol and Lago Lepué.

Radiocarbon dates of organic material from the base of cores through lacustrine sediments that overlie glacial deposits situated on the continent in areas formerly covered by the Golfo de Corcovado and Seno Reloncaví glacier lobes indicate that rapid glacier recession followed the youngest advance into the LGM moraine belt. A series of radiocarbon dates from a roadside outcrop just north of the Chaitén township (site 34 in Fig. 1) shows a sequence of ages in stratigraphic order through an organic mud unit that directly overlies glaciofluvial deposits. The lowest of these dates, at the base of the organic unit, yielded a minimum-limiting age of 13,830 ± 50 $^{14}$C yrs BP (16,737 ± 125 cal yrs BP) (Supplementary Table 3) for recession of the Golfo de Corcovado ice lobe ~80 km upstream from the Lago Lepué site. A sequence of radiocarbon dates throughout two low-elevation stratigraphic sections in the Andean foothills about 35 and 40 km inboard of Punta Penas (site 24 in Fig. 1) afford close minimum-limiting ages for recession of the Seno Reloncaví ice lobe at 14,070 ± 35 $^{14}$C yrs BP (17,107 ± 99 cal yrs BP; Supplementary Table 3) at Caleta Puelche (site 35 in Fig. 1) and 13,670 ± 40 $^{14}$C yrs BP (16,486 ± 110 cal yrs BP; Supplementary Table 3) at Lago Pröschle (site 36 in Fig. 1) (Supplementary Table 3). Organic sediments deposited in Lago Reflejos (site 37 in Fig. 1), situated on a lateral moraine/kame complex at 800 m elevation, yielded a basal age of 13,740 ± 60 $^{14}$C yrs BP (16,600 ± 138 cal yrs BP) (Supplementary Table 3) for the transition from laminated glaciolacustrine mud in the bottom of a 360-cm-long sediment core to organic-rich lacustrine sectors of the core. Lago Reflejos lies within a kilometer of an abandoned cirque, at the head of an 11-km-long glacial valley that held a tributary glacier of the Seno Reloncaví ice lobe when it extended to the inner ice-contact slope of the LGM moraine belt. Thus low-and-high-elevation areas well inboard of the Seno Reloncaví LGM moraines were ice-free by ~13,700 $^{14}$C yrs BP (~16,700 cal yrs BP).

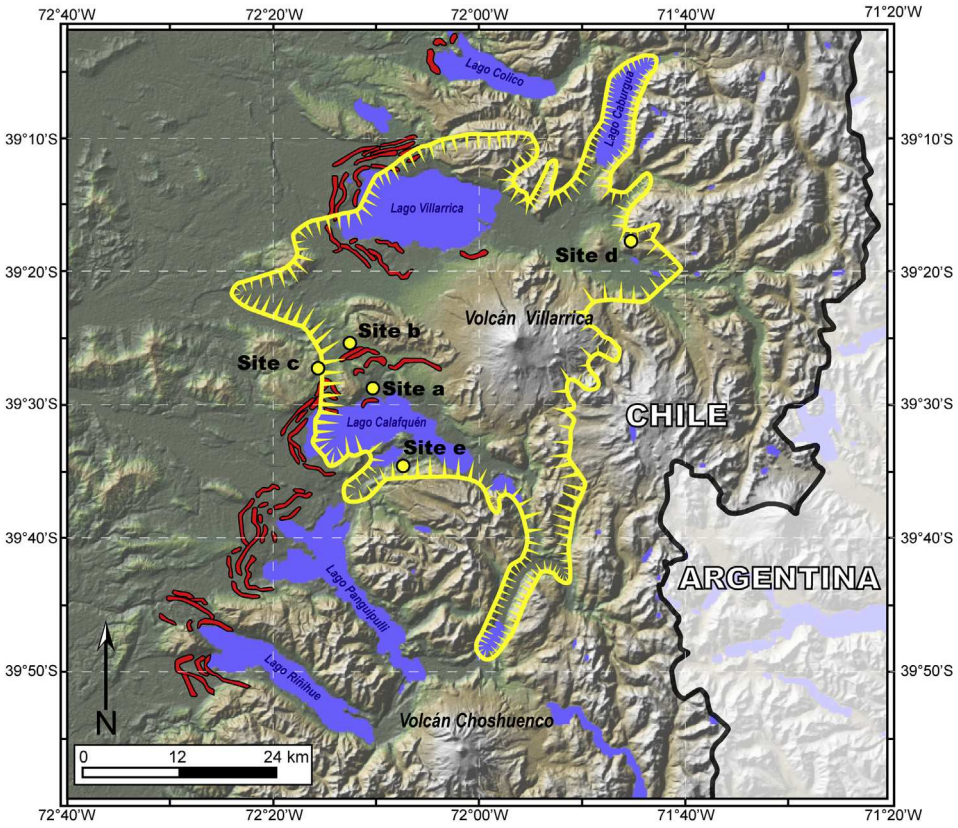


**Fig. 9.** Detail of the Volcán Villarrica area showing the extent of the Licán ignimbrite (polygon delimited with the yellow line), glacial limits during the LGM outboard of the western ends of the lakes (moraine crests depicted with red lines), and location of radiocarbon-dated samples of charcoal from exposures in the Licán ignimbrite and Cudico pyroclastic sediments (see Supplementary Table 3 for details on the radiocarbon dates). (For interpretation of the references to colour in this figure legend, the reader is referred to the web version of this article.)

The age of the initial recession of the Rupanco piedmont lobe during the LGT is revealed in sediment cores from the small Laguna Bonita inter-morainal depression south of Lago Rupanco (site 38 in Fig. 1). Laguna Bonita is bounded by the outermost Llanquihue-age moraine belt along its southern margin and by a younger Llanquihue-age moraine complex along its northern edge. Piston cores collected from the deepest part of the basin show an abrupt transition from laminated glaciolacustrine mud to organic-rich lake sediments, suggesting that a small ice-dammed lake occupied the basin when the Rupanco lobe deposited the younger moraine complex along the northern edge of Laguna Bonita. The end of glaciolacustrine sedimentation occurred when the Rupanco ice front abandoned these moraines and deposition of organic lake sediments commenced in Laguna Bonita shortly before 14,507 ± 82 $^{14}$C yrs BP (17,685 ± 120 cal yrs BP) (Supplementary Tables 2 and 3).

### 4.3. Distribution and age of the Licán ignimbrite

The timing and areal distribution of deposits from Volcán Villarrica (39°25′0″S, 71°56′0″W, 2847 m asl) (Fig. 1), the most active volcano of the Southern Andean Volcanic Zone, also document glacier recession early in the LGT. The Villarrica edifice has a volume of about 250 km$^3$ and its eruptive products cover more than 700 km$^2$ of the surrounding terrain (Moreno, 1993). Eruptive activity since the LGM produced basalt and basaltic andesite lava flows, along with pyroclastic flow deposits. Volcán Villarrica has generated several large explosive eruptions, which early in the LGT led to the emplacement of the Cudico pyroclastic flow sediments and the Licán ignimbrite. Of these, the Licán ignimbrite (Figs. 1 and 10) is the most extensive, with deposits found ~40 km from the source and over an area of more than 1000 km$^2$ surrounding the volcano. Details on the geochemistry, stratigraphy, and distribution of these deposits can be found in Clavero and Moreno (2004) and Lohmar et al. (2007).

The Villarrica and Calafquén piedmont glacier lobes, located in the northern part of the Chilean Lake District (~39°30′S, ~72°W), formed well-defined arcuate moraine systems and extensive outwash plains west of their respective lake basins during the Llanquihue glaciation (Laugenie, 1982) (Figs. 1 and 10). The Licán ignimbrite not only mantles the LGM moraines but, of key importance for this study, it also extends as tongues well into Andean valleys (Clavero and Moreno, 2004) that fed the Lago Villarrica and Calafquén piedmont glacier lobes when they extended to their respective Llanquihue limits. Depicted in Fig. 9, this footprint shows that glaciers had already receded deep into the Andes by the time the Licán ignimbrite was deposited. We collected samples of charcoal from within the ignimbrite at the five sites lettered in Fig. 9 (Supplementary Table 3). The resulting radiocarbon dates are tightly constrained and yielded a mean value (±1σ) of 13,847 ± 77 $^{14}$C yrs BP (16,761 ± 113 cal yrs BP) (Supplementary Table 2). In addition, at site b in Fig. 9, sediments of the Cudico pyroclastic flow crop out on the land surface beneath the Licán ignimbrite. A charcoal sample collected from Cudico flow sediments gave a date of 13,880 ± 100 $^{14}$C yrs BP (16,808 ± 178 cal yrs BP). Taken together, the age and footprint of the Licán ignimbrite indicate extensive deglaciation of the Andes in the northern Chilean Lake District prior to 13,846 ± 28 $^{14}$C yrs BP (16,761 ± 109 cal yrs BP).

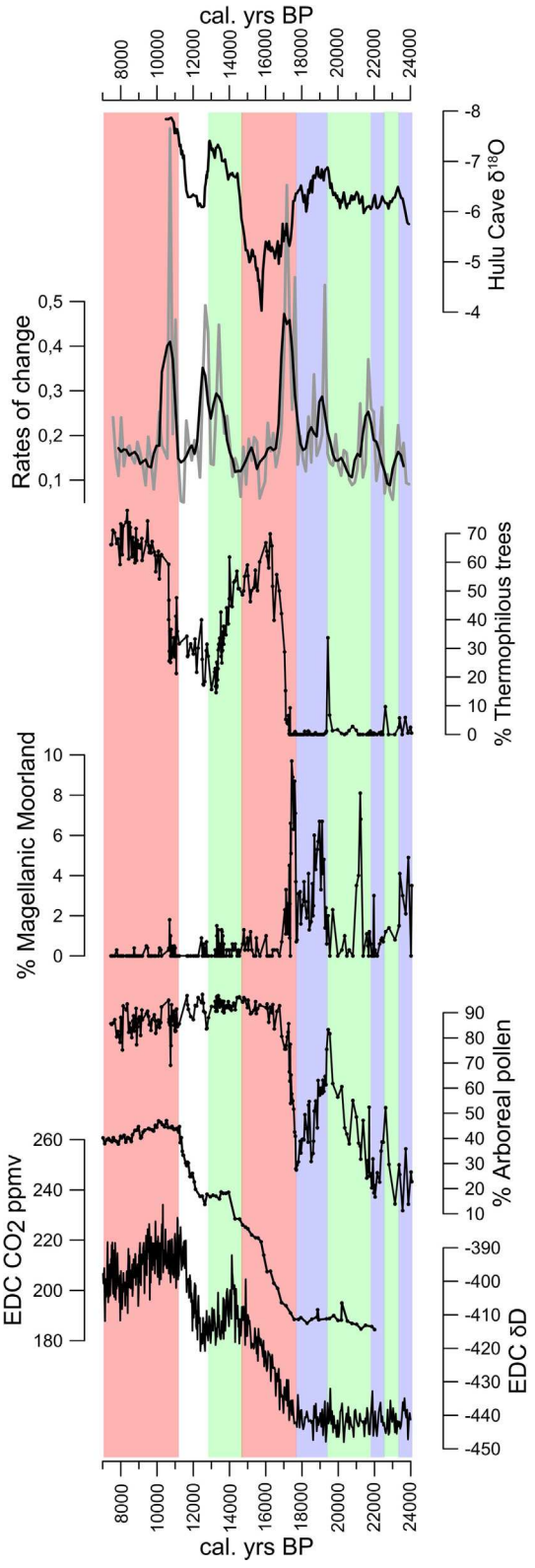


**Fig. 10.** Summary of the paleovegetation record shown in this paper compared with the $CO_2$ and δD records from EPICA Dome C East Antarctica (Monnin et al., 2001; Stenni et al., 2003) and the $\delta^{18}O$ record from Hulu Cave, China (Wang et al., 2001). The vertical blue bars represent extreme glacial conditions, green bars represent cold-temperate conditions, red bars represent warm conditions, see text for discussion on the interpretation of the pollen record. The portion of the record dated between ~11,000–13,000 cal yrs BP, shown without color, corresponds to an interval of intense fire activity and disturbance of the rainforest vegetation under cold-temperate conditions and a highly variable precipitation regime. (For interpretation of the references to colour in this figure legend, the reader is referred to the web version of this article.)

## 5. Discussion

Our radiocarbon chronology documents recurrent expansions of Patagonian ice sheet piedmont lobes into the Chilean Lake District and Isla Grande de Chiloé at ~33,600, ~30,800, ~26,900, and ~26,000 cal yrs BP. The youngest advance into the Llanquihue moraine belt took place between ~17,700 and 18,100 cal yrs BP. The culmination of this advance was followed immediately by recession deep into the Andes by at least ~16,800 cal yrs BP, if not earlier, as documented by the distribution and age of the Licán ignimbrite, as well as by minimum-limiting basal radiocarbon dates recording ice-free conditions in the eastern mountainous region of the mainland and in the Chiloé Continental sector. Thus the glacial geologic data from the Chilean Lake District show recurring glacial conditions from at least as early as ~33,600 until ~17,800 cal yrs BP, after which time the northwest sector of the Patagonian Ice Sheet underwent extensive recession in response to sustained atmospheric warming (Fig. 10).

The palynological records from Canal de la Puntilla and Huelmo add further support to climatic inferences derived from the glacial geologic record. Pollen-inferred vegetation changes reconstructed from these locations indicate cold and wet glacial conditions between ~17,800 and 24,000 cal yrs BP, punctuated by millennial-scale cooling intervals at ~23,400 – 24,000, ~22,600 – 23,400, and ~17,800 – 19,300 cal yrs BP. A brief reversion from cold to warm conditions that began around 22,600 cal yrs BP and peaked at 19,300 cal yrs BP corresponds in timing with the Varas Interstade, a period of muted glacial activity prior to the last major advance into the Llanquihue moraine belts (Denton et al., 1999b; Mercer, 1972). The abundance of Magellanic Moorland species increased during the cold interval dated between ~17,800 and 19,300 cal yrs BP, contemporaneous with the youngest glacial advance into the Llanquihue moraine belt at ~18,000 cal yrs BP (Fig. 10).

An abrupt increase in *N. dombeyi* type at ~17,800 cal yrs BP records the onset of rapid warming at the end of the last glacial period in northwest Patagonia. The chronology for this event is identical within dating uncertainties to the beginning of glacier recession of multiple ice lobes from their final position in the Llanquihue moraine belts between 41° and 43°S in northwestern Patagonia (Fig. 1, Supplementary Table 3). Magellanic Moorland species disappeared at ~17,300 cal yrs BP implying a shift from hyperhumid to humid conditions, signaling a poleward displacement of the southern westerly wind belt shortly after the beginning of the LGT.

Thermophilous North Patagonian trees appeared at ~17,100 cal yrs BP and increased rapidly, leading to the establishment of closed-canopy rainforests by ~16,800 cal yrs BP. These episodes of arboreal expansion were rapid events, as revealed by the rates-of-parameter, suggesting that large-scale warming brought full glacial climate to average Holocene conditions within ~1000 years after the onset of deglaciation. The overall implication of this finding is that abrupt warming commencing at ~17,800 cal yrs BP led to an extraordinarily fast vegetation turnover event, along with extensive and rapid deglaciation in northwestern Patagonia, as revealed by the distribution and age of the Licán ignimbrite and the onset of ice-free conditions in the Andes of the mainland and the lowlands of Chiloé continental. Our estimate of at least ~750 m rise in the regional treeline along with ice-free conditions up to 800 m.a.s.l. in Andean cirques following the onset of the LGT, suggest that 75–80% of the glacial-interglacial temperature recovery took place within ~1000 years after the demise of the LGM.

Extensive glacier recession in northwestern Patagonia between ~17,800 and ~16,800 yrs BP was coeval with deglaciation in the southern sector of the Patagonian Ice Sheet (Fig. 10). The east-

flowing outlet glacier occupying the Lago Argentino trough at 50°S had retreated well up valley to within late-glacial limits, as defined by the Puerto Bandera moraine belt, by at least as early as 13,450 ± 150 $^{14}$C yrs BP (16,200 ± 230 yrs BP; recalibrated with INTCAL13) (Strelin et al., 2011). In southernmost Patagonia at Tierra del Fuego (54–55°S), glaciers had receded from LGM limits to near-present-day margins in Cordillera Darwin by as early as 13,650 ± 90 $^{14}$C yrs BP (16,500 ± 160 cal yrs BP, recalibrated with INTCAL13) (Hall et al., 2013), and close to the late-glacial limit in small glacial cirques north of the Beagle Channel by 16,950 ± 750 cal yrs BP (Menounos et al., 2013). Thus atmospheric warming and deglaciation by ~16,500 cal yrs BP occurred across 16° of latitude in southern South America from 39°S to 55°S.

We identify a cooling trend that featured increased precipitation between ~13,000 – 14,700 cal yrs BP, and intense fire activity between ~12,000 – 13,000 cal yrs BP, suggesting that millennial-scale variations in the southern westerly winds were superimposed upon this temperature reversal. Available chronologies from southwestern Patagonia indicate advance of the Río Paine glacier lobe in Torres del Paine between ~12,600 and 14,800 cal yrs BP (Garcia et al., 2012; Moreno et al., 2009) and deposition of the Puerto Banderas moraine in Lago Argentino at ~ 12,990 cal yrs BP (Strelin et al., 2011). Ice recession ensued, reaching sectors inboard of the Holocene moraines in the Lago Argentino area prior to 7700 cal yrs BP (Strelin et al., 2014). These data suggest colder and wetter conditions during the Antarctic Cold Reversal (ACR) and wet/dry anomalies in precipitation in southwestern/northwestern Patagonia during Younger Dryas (YD) time, implying stronger southern westerly winds along 10° of latitude followed by a southward shift, respectively (Moreno et al., 2012). These changes were contemporaneous with renewed glacial activity in southwestern Patagonia during the ACR and recession during YD time.

The timing of Patagonian deglaciation and vegetation change was mirrored on the opposite side of the South Pacific Ocean in the Southern Alps of New Zealand. Extensive glacier recession from LGM limits in the Rakaia valley, located at 44°S in the central Southern Alps, occurred between 17,840 ± 240 and 15,660 ± 160 years ago (Putnam et al., 2013). Glaciological modeling indicates that this recession was driven by a 4.5 °C increase in summer atmospheric temperature, which accounts for 86% of the full glacial-to-early Holocene temperature rise (Putnam et al., 2013). Furthermore, pollen records in New Zealand mirror those in South America and show the onset of rapid deglacial vegetation changes at ~17,890 cal yrs BP. On North Island, the deposition of the Rerewhakaaitu tephra at 17,890 ± 130 cal yrs BP (based on an error-weighted mean radiocarbon age of 14,700 ± 95 $^{14}$C yrs BP in terrestrial records) coincided with the replacement of subalpine flora by tall *Podocarpus* trees indicative of a warmer climate, thereby providing a marker of the onset of the LGT (Newnham et al., 2003). At the same time on South Island, a landscape dominated by grasses was rapidly converted to scrubland and then forest between ~17,000 and ~18,000 cal yrs BP (Vandergoes et al., 2013).

Taken together, mountain glacier systems and vegetation assemblages on opposite sides of the South Pacific document a profound warming that brought a rapid end to the last ice age in Southern Hemisphere middle latitudes. Widespread warming commenced sharply ~17,800 years ago and near-interglacial conditions were achieved ~1000 years later. Therefore any explanation for what drove the last glacial termination must account for such decisive, widespread, and nearly complete glacial-to-interglacial warming registered across a wide latitudinal band of the Southern Hemisphere between 16,800 and 17,800 cal yrs BP.

One such explanation for the signature of southern mid-latitude deglacial warming could involve the far-field effects of Heinrich Stadial 1 in the North Atlantic region. Heinrich Stadial 1 featured curtailed overturning and strong winter-centric cooling of the North Atlantic (Bard et al., 2000; McManus et al., 2004), weakening of Asian Monsoons (Dykoski et al., 2005; Wang et al., 2001), a coupled southward shift of the Intertropical Convergence Zone and Southern Hemisphere westerlies (Anderson et al., 2009; Chiang et al., 2014), and progressive destratification of the Southern Ocean (Anderson et al., 2009; Burke and Robinson). The onset of Heinrich Stadial 1 coincided closely with the initiation of deglaciation in Patagonia and New Zealand, abrupt switches from cryophilic to thermophyllic vegetation assemblages in those regions, and sustained temperature and atmospheric $CO_2$ increments revealed in Antarctic ice cores (Members, 2015; Monnin et al., 2001; Stenni et al., 2003). Interglacial conditions were achieved in southern middle latitudes midway through Heinrich Stadial 1, unlike ice core records from Antarctica (Members, 2015; Stenni et al., 2003). Therefore a strong possibility is that Southern Hemispheric warming and deglaciation were closely linked to Heinrich Stadial 1, implying a fundamental role for Heinrich Stadials in terminating glacial conditions in Southern Hemisphere middle latitudes.

## 6. Conclusions

- Recurrent expansions of the Patagonian ice sheet occurred at ~33,600, ~30,800, ~26,900, and ~26,000 cal yrs BP into the lowlands of the Chilean Lake District and Isla Grande de Chiloé.
- Stratigraphic, geomorphic, and palynologic evidence from northwestern Patagonia indicate that the final LGM advance of Andean ice lobes took place between ~17,700 and 18,100 cal yrs BP during a cold wet episode between ~17,800 and 19,300 cal yrs BP.
- Deglacial warming that began at ~17,800 cal yrs BP led to expansion of North Patagonian rainforest species and the abrupt withdrawal of Andean ice lobes. Glacial recession was abrupt, reaching deep into Andean valleys within ~1000 years. Thus, two entirely independent temperature sensitive proxies document rapid warming from full-glacial to near-interglacial conditions occurred between 17,800 and 16,800 cal yrs BP.
- Mid- and high-latitude paleoclimate data from the Southern Hemisphere indicate that the ~17,800 cal yrs BP warm pulse was a decisive trigger for the last glacial termination.
- Magellanic Moorland species disappeared at ~17,300 cal yrs BP, attesting to a shift from hyperhumid to humid conditions driven by a poleward displacement of the southern westerly wind belt shortly after the beginning of the last glacial termination.

## Acknowledgments

We thank J. Muñoz and R. Flores from Servicio Nacional de Geología y Minería for field logistics, I. Hajdas, C.M. Moy and T. Guilderson for their contribution toward the development of our radiocarbon chronology. P.I.M. acknowledges support from Fondecyt grants 1110612, 1131055, ICM grants P05-002 and NC120066, and Fondap 15110009. M.R. Kaplan was supported by the Comer Science and Educational Foundation and NSF-BCS award 12-63474. A.E. Putnam was supported by a Lamont Postdoctoral Fellowship, the Comer Science and Education Foundation, and the Lenfest Foundation. G.H. Denton was supported by the U.S. National Science Foundation. This is LDEO contribution #7906

## Appendix A. Supplementary data

Supplementary data related to this article can be found at http://dx.doi.org/10.1016/j.quascirev.2015.05.027.

## References


Abarzua, A.M., Moreno, P.I., 2008. Changing fire regimes in the temperate rainforest region of southern Chile over the last 16,000 yr. Quat. Res. 69, 62–71.

Aceituno, P., Fuenzalida, H., Rosenbluth, 1993. Climate along the extratropical west coast of South America. In: Mooney, Fuentes, Kromberg (Eds.), Earth Systems Responses to Global Change. Academic press, pp. 61–70.

Andersen, B.G., Denton, G.H., Lowell, T.V., 1999. Glacial geomorphologic maps of the Llanquihue drift in the area of the Southern Lake District, Chile. Geogr. Ann. Ser. A Phys. Geogr. 81A, 155–166.

Anderson, R.F., Ali, S., Bradtmiller, L.I., Nielsen, S.H.H., Fleisher, M.Q., Anderson, B.E., Burckle, L.H., 2009. Wind-driven upwelling in the southern ocean and the deglacial rise in atmospheric CO2. Science 323, 1443–1448.

Bard, E., Rostek, F., Turon, J.-L., Gendreau, S., 2000. Hydrological impact of Heinrich events in the subtropical northeast Atlantic. Science 289, 1321–1324.

Bennett, K.D., Haberle, S.G., Lumley, S.H., 2000. The last glacial-Holocene transition in Southern Chile. Science 290, 325–328.

Blaauw, M., Christen, J.A., 2011. Flexible paleoclimate age-depth models using an autoregressive gamma process. Bayesian Anal. 6, 457–474.

Bronk Ramsey, C., 2009. Bayesian analysis of radiocarbon dates. Radiocarbon 51, 337–360.

Burke, A., Robinson, L.F., 2012. The southern Ocean's role in Carbon Exchange during the last deglaciation. Science 335, 557–561.

Clavero, J., Moreno, H., 2004. Evolution of Villarrica Volcano. In: Lara, L., C, A.J. (Eds.), Villarrica Volcano (39.5°S), Southern Andes, Chile. Servicio Nacional de Geología y Minería, Santiago, pp. 17–27.

Condom, T., Coudrain, A., Sicart, J.E., Thery, S., 2007. Computation of the space and time evolution of equilibrium-line altitudes on Andean glaciers (10 degrees N-55 degrees S). Glob. Planet. Change 59, 189–202.

Chiang, J.C.H., Lee, S.Y., Putnam, A.E., Wang, X.F., 2014. South Pacific Split Jet, ITCZ shifts, and atmospheric North-South linkages during abrupt climate changes of the last glacial period. Earth Planet. Sci. Lett. 406, 233–246.

Clark, P.U., Dyke, A.S., Shakun, J.D., Carlson, A.E., Clark, J., Wohlfarth, B., Mitrovica, J.X., Hostetler, S.W., McCabe, A.M., 2009. The Last Glacial Maximum. Science 325, 710–714.

Denton, G.H., Heusser, C.J., Lowell, T.V., Moreno, P.I., Andersen, B.G., Heusser, L.E., Schluchter, C., Marchant, D.R., 1999a. Interhemispheric linkage of paleoclimate during the last glaciation. Geogr. Ann. Ser. a-Physical Geogr. 81A, 107–153.

Denton, G.H., Lowell, T.V., Heusser, C.J., Schluchter, C., Andersen, B.G., Heusser, L.E., Moreno, P.I., Marchant, D.R., 1999b. Geomorphology, stratigraphy, and radiocarbon chronology of Llanquihue drift in the area of the southern Lake District, Seno Reloncavi, and Isla Grande de Chiloe, Chile. Geogr. Ann. Ser. A Phys. Geogr. 81A, 167–229.

Dykoski, C.A., Edwards, R.L., Cheng, H., Yuan, D.X., Cai, Y.J., Zhang, M.L., Lin, Y.S., Qing, J.M., An, Z.S., Revenaugh, J., 2005. A high-resolution, absolute-dated Holocene and deglacial Asian monsoon record from Dongge Cave, China. Earth Planet. Sci. Lett. 233, 71–86.

Fletcher, M.S., Moreno, P.I., 2012. Have the Southern Westerlies changed in a zonally symmetric manner over the last 14,000 years? A hemisphere-wide take on a controversial problem. Quat. Int. 253, 32–46.

Garcia, J.L., Kaplan, M.R., Hall, B.L., Schaefer, J.M., Vega, R.M., Schwartz, R., Finkel, R., 2012. Glacier expansion in southern Patagonia throughout the Antarctic cold reversal. Geology 40, 859–862.

Garreaud, R., Lopez, P., Minvielle, M., Rojas, M., 2013. Large-scale control on the patagonian climate. J. Clim. 26, 215–230.

Gonzalorena, L.A., 2015. Historia postglacial de la vegetación de Lago Tarumán en la zona centro-occidental de Isla Grande de Chiloé: inferencias paleoambientales a partir de un registro palinológico de alta resolución. Departamento de Ciencias Ecológicas. Universidad de Chile, Santiago.

Hajdas, I., Bonani, G., Moreno, P.I., Ariztegui, D., 2003. Precise radiocarbon dating of late-glacial cooling in mid-latitude South America. Quat. Res. 59, 70–78.

Hall, B.L., Porter, C.T., Denton, G.H., Lowell, T.V., Bromley, G.R.M., 2013. Extensive recession of cordillera Darwin glaciers in southernmost south america during heinrich stadial 1. Quat. Sci. Rev. 62, 49–55.

Heusser, C.J., 1974. Vegetation and climate of the southern Chilean lake district during and since the last Interglaciation. Quat. Res. 4, 190–315.

Heusser, C.J., 1990. Late-glacial and holocene vegetation and climate of Sub-Antarctic South-America. Rev. Palaeobot. Palynol. 65, 9–15.

Heusser, C.J., Heusser, L.E., Lowell, T.V., 1999. Paleoecology of the southern Chilean Lake District- Isla Grande de Chiloé during middle-Late Llanquihue glaciation and deglaciation. Geogr. Ann. Ser. A Phys. Geogr. 81 A, 231–284.

Heusser, C.J., Lowell, T.V., Heusser, L.E., Hauser, A., Andersen, B.G., Denton, G.H., 1996a. Full-glacial-late-glacial paleoclimate of the Southern Andes: evidence from pollen, beetle, and glacial records. J. Quat. Sci. 11, 173–184.

Heusser, C.J., Lowell, T.V., Heusser, L.E., Hauser, A., Andersen, B.G., Denton, G.H., 1996b. Full-glacial – late-glacial palaeoclimate of the Southern Andes: evidence from pollen, beetle, and glacial records. J. Quat. Sci. 11, 173–184.

Holz, A., Veblen, T.T., 2012. Wildfire activity in rainforests in western Patagonia linked to the Southern Annular Mode. Int. J. Wildland Fire 21, 114–126.

Jara, I.A., Moreno, P.I., 2012. Temperate rainforest response to climate change and disturbance agents in northwestern Patagonia (41 degrees S) over the last 2600 years. Quat. Res. 77, 235–244.

Lara, A., Villalba, R., Wolodarsky-Franke, A., Aravena, J.C., Luckman, B.H., Cuq, E., 2005. Spatial and temporal variation in Nothofagus pumilio growth at tree line along its latitudinal range (35 degrees 40 '-55 degrees S) in the Chilean Andes. J. Biogeogr. 32, 879–893.

Laugenie, C., 1982. La région des lacs, Chili mériodonal, recherches sur l'évolution géomorphologique d'un piédemont glaciaire quaternaire andin, Volume I. Université de Bordeaux, p. 332. Volume II (822 pp.).

Lowell, T.V., Heusser, C.J., Andersen, B.G., Moreno, P.I., Hauser, A., Heusser, L.E., Schluchter, C., Marchant, D.R., Denton, G.H., 1995. Interhemispheric correlation of late Pleistocene glacial events. Science 269, 1541–1549.

Lliboutry, L., 1998. Glaciers of Chile and Argentina. In: Williams, R.S., Ferrigno, J.G. (Eds.), Satellite Image Atlas of Glaciers of the World: South America. USGS Professional Paper 1386-I, Online version 1.02.

Lohmar, S., Robin, C., Gourgaud, A., Clavero, J., Parada, M.A., Moreno, H., Ersoy, O., Lopez-Escobar, L., Naranjo, J.A., 2007. Evidence of magma-water interaction during the 13,800 years BP explosive cycle of the Lican Ignimbrite, Villarrica volcano (southern Chile). Rev. Geol. Chile 34, 233–247.

McManus, J.F., Francois, R., Gherardi, J.-M., Keigwin, L.D., Brown-Leger, S., 2004. Collapse and rapid resumption of Atlantic meridional circulation linked to deglacial climate changes. Nature 428, 834–837.

Members, W.D.P., 2015. Precise interpolar phasing of abrupt climate change during the last ice age. Nature 520, 661–665.

Menounos, B., Clague, J.J., Osborn, G., Davis, P.T., Ponce, F., Goehring, B., Maurer, M., Rabassa, J., Coronato, A., Marr, R., 2013. Latest Pleistocene and Holocene glacier fluctuations in southernmost Tierra del Fuego, Argentina. Quat. Sci. Rev. 77, 70–79.

Mercer, J.H., 1968. Variations of some Patagonian glaciers since the Late-Glacial. Am. J. Sci. 266, 91–109.

Mercer, J.H., 1972. Chilean glacial chronology 20,000 to 11,000 Carbon-14 years ago: some global comparisons. Science 172, 1118–1120.

Mercer, J.H., 1976. Glacial history of southernmost South America. Quat. Res. 6, 125–166.

Monnin, E., Indermuhle, A., Dallenbach, A., Fluckiger, J., Stauffer, B., Stocker, T.F., Raynaud, D., Barnola, J.M., 2001. Atmospheric $CO_2$ concentrations over the last glacial termination. Science 291, 112–114.

Moreno, P.I., 1997. Vegetation and climate near Lago Llanquihue in the Chilean Lake District between 20200 and 9500 C-14 yr BP. J. Quat. Sci. 12, 485–500.

Moreno, P.I., 2004. Millennial-scale climate variability in northwest Patagonia over the last 15000 yr. J. Quat. Sci. 19, 35–47.

Moreno, P.I., Francois, J.P., Villa-Martínez, R., Moy, C.M., 2010. Covariability of the Southern Westerlies and atmospheric CO2 during the Holocene. Geology 39, 727–730.

Moreno, P.I., Jacobson, G.L., Andersen, B.G., Lowell, T.V., Denton, G.H., 1999. Abrupt vegetation and climate changes during the last glacial maximum and the last termination in the Chilean Lake District: a case study from Canal de la Puntilla (41°S). Geogr. Ann. Ser. A Phys. Geogr. 81 A, 285–311.

Moreno, P.I., Jacobson, G.L., Lowell, T.V., Denton, G.H., 2001. Interhemispheric climate links revealed by a late-glacial cooling episode in southern Chile. Nature 409, 804–808.

Moreno, P.I., Kaplan, M.R., Francois, J.P., Villa-Martinez, R., Moy, C.M., Stern, C.R., Kubik, P.W., 2009. Renewed glacial activity during the Antarctic cold reversal and persistence of cold conditions until 11.5 ka in southwestern Patagonia. Geology 37, 375–378.

Moreno, P.I., Leon, A.L., 2003. Abrupt vegetation changes during the last glacial to Holocene transition in mid-latitude South America. J. Quat. Sci. 18, 787–800.

Moreno, P.I., Villa-Martinez, R., Cardenas, M.L., Sagredo, E.A., 2012. Deglacial changes of the southern margin of the southern westerly winds revealed by terrestrial records from SW Patagonia (52 degrees S). Quat. Sci. Rev. 41, 1–21.

Newnham, R.M., Eden, D.N., Lowe, D.J., Hendy, C.H., 2003. Rerewhakaaitu Tephra, a land-sea marker for the Last Termination in New Zealand, with implications for global climate change. Quat. Sci. Rev. 22, 289–308.

Pesce, O.H., Moreno, P.I., 2014. Vegetation, fire and climate change in central-east Isla Grande de Chiloé (43°S) since the Last Glacial Maximum, northwestern Patagonia. Quat. Sci. Rev. 90, 143–157.

Porter, S.C., 1981. Pleistocene glaciation in the southern lake district of Chile. Quat. Res. 16, 263–292.

Putnam, A.E., Schaefer, J.M., Denton, G.H., Barrell, D.J.A., Andersen, B.G., Koffman, T.N.B., Rowan, A.V., Finkel, R.C., Rood, D.H., Schwartz, R., Vandergoes, M.J., Plummer, M.A., Brocklehurst, S.H., Kelley, S.E., Ladig, K.L., 2013. Warming and glacier recession in the Rakaia valley, Southern Alps of New Zealand, during Heinrich Stadial 1. Earth Planet. Sci. Lett. 382, 98–110.

Quintana, J.M., Aceituno, P., 2012. Changes in the rainfall regime along the extra-tropical west coast of South America (Chile): 30-43 degrees S. Atmosfera 25, 1–22.

Singer, B.S., Jicha, B.R., Harper, M.A., Naranjo, J.A., Lara, L.E., Moreno-Roa, H., 2008. Eruptive history, geochronology, and magmatic evolution of the Puyehue-Cordon Caulle volcanic complex, Chile. Geol. Soc. Am. Bull. 120, 599–618.

Stenni, B., Jouzel, J., Masson-Delmotte, V., Rothlisberger, R., Castellano, E., Cattani, O., Falourd, S., Johnsen, S.J., Longinelli, A., Sachs, J.P., Selmo, E., Souchez, R., Steffensen, J.P., Udisti, R., 2003. A late-glacial high-resolution site and source temperature record derived from the EPICA Dome C isotope records (East Antarctica). Earth Planet. Sci. Lett. 217, 183–195.

Stern, C., 2004. Active Andean volcanism: its geologic and tectonic setting. Rev. Geol. Chile 31, 161–206.

Strelin, J.A., Denton, G.H., Vandergoes, M.J., Ninnemann, U.S., Putnam, A.E., 2011. Radiocarbon chronology of the late-glacial puerto Bandera moraines, southern patagonian Icefield, Argentina. Quat. Sci. Rev. 30, 2551–2569.
Strelin, J.A., Kaplan, M.R., Vandergoes, M.J., Denton, G.H., Schaefer, J.M., 2014. Holocene glacier history of the Lago Argentino basin, Southern Patagonian Icefield. Quat. Sci. Rev. 101, 124–145.
Vandergoes, M.J., Newnham, R.M., Denton, G.H., Blaauw, M., Barrell, D.J.A., 2013. The anatomy of Last Glacial Maximum climate variations in south Westland, New Zealand, derived from pollen records. Quat. Sci. Rev. 74, 215–229.
Veblen, T.T., Donoso, C., Kitzberger, T., Rebertus, A.J., 1996. Ecology of the southern Chilean and Argentinean Nothofagus forests. In: Veblen, T.T., Hill, R.S., Read, J. (Eds.), The Ecology and Biogeography of Nothofagus Forests. Yale University Press, New Haven, pp. 293–353.
Villa-Martinez, R., Moreno, P.I., Valenzuela, M.A., 2012. Deglacial and postglacial vegetation changes on the eastern slopes of the central Patagonian Andes (47 degrees S). Quat. Sci. Rev. 32, 86–99.
Villagrán, C., 1985. Análisis palinológico de los cambios vegetacionales durante el Tardiglacial y Postglacial en Chiloé, Chile. Rev. Chil. Hist. Nat. 58, 57–69.
Villagrán, C., 1988a. Expansion of Magellanic moorland during the Late Pleistocene: palynological evidence from northern Isla Grande de Chiloé, Chile. Quat. Res. 30, 304–314.
Villagrán, C., 1988b. Late Quaternary vegetation of Southern Isla Grande de Chiloé, Chile. Quat. Res. 29, 294–306.
Villagrán, C., 1990. Glacial, Late-Glacial, and Post-Glacial climate and vegetation of the Isla Grande de Chiloé, Southern Chile (41–44°S). Quat. S. Am. Antarct. Penins. 8, 1–15.
Villagrán, C., 2001. Un modelo de la historia de la vegetación de la Cordillera de la Costa de Chile central-sur: la hipótesis glacial de Darwin. Rev. Chil. Hist. Nat. 74, 793–803.
Wang, Y.J., Cheng, H., Edwards, R.L., An, Z.S., Wu, J.Y., Shen, C.C., Dorale, J.A., 2001. A high-resolution absolute-dated Late Pleistocene monsoon record from Hulu Cave, China. Science 294, 2345–2348.